Bratislava Medical Journal (2026) 127:2199–2221
https://doi.org/10.1007/s44411-026-00579-1

RESEARCH

Red Beet (*Beta vulgaris*) Extract and Betanin Attenuate Valproic Acid–Induced Autism-Like Neurobehavioral and Molecular Alterations via Modulation of Oxidative Stress, Neuroinflammation, Apoptosis, and Reelin Signaling

Nada S. Al-wakeel[1] · Manar E. Selim[2] · Yasmina M. Abd-Elhakim[3] · Manal M. Hefny[1]

Received: 11 November 2025 / Revised: 7 December 2025 / Accepted: 9 March 2026 / Published online: 9 April 2026
© The Author(s) 2026

Abstract

Autism spectrum disorder (ASD) is a complex neurodevelopmental condition linked to social-communication and behavioral impairments, with emerging evidence implicating oxidative stress, neuroinflammation, and disrupted neurotransmission in its pathogenesis. Natural compounds with antioxidant and anti-inflammatory potential are explored as alternative therapeutic agents. This study investigated the neuroprotective effects of *Beta vulgaris* leaf ethanolic extract and its bioactive compound, betanin, in a rat model of ASD induced by prenatal valproic acid (VPA) exposure. Male neonatal rats, born to dams prenatally exposed to VPA (400 mg/kg b.wt on E12.5), were postnatally (PND 23 to PND 37) treated with either water (VPA/W), extract solvent (VPA/SE), *B. vulgaris* extract (200 mg/kg b.wt, VPA/EE), or betanin (25 mg/kg b.wt, VPA/BT), and compared to rats from control dams that received the same postnatal treatments (CW, CSE, CEE, and CBT, respectively). Behavioral assessments showed that VPA/EE and VPA/BT significantly improved sociability and social novelty deficits. Biochemical analyses revealed that both treatments enhanced GABA levels, reduced oxidative stress markers (MDA), elevated antioxidant defenses (GSH and CAT), and decreased pro-inflammatory TNF-α. Apoptotic markers (BCL2 and Caspase-3) were normalized, and histopathological brain abnormalities were ameliorated. Also, Reelin gene expression, suppressed by VPA, was significantly upregulated following treatment. While VPA/BT showed greater efficacy in improving sociability and neurotransmitter balance, VPA/EE exhibited broader molecular modulation. These findings concluded that *B. vulgaris* extract and betanin possess substantial neuroprotective properties via antioxidant, anti-inflammatory, anti-apoptotic, and neuromodulatory pathways. Their potential as adjunctive treatments for ASD warrants further clinical investigation.

✉ Manar E. Selim
manar.efat@gu.edu.eg

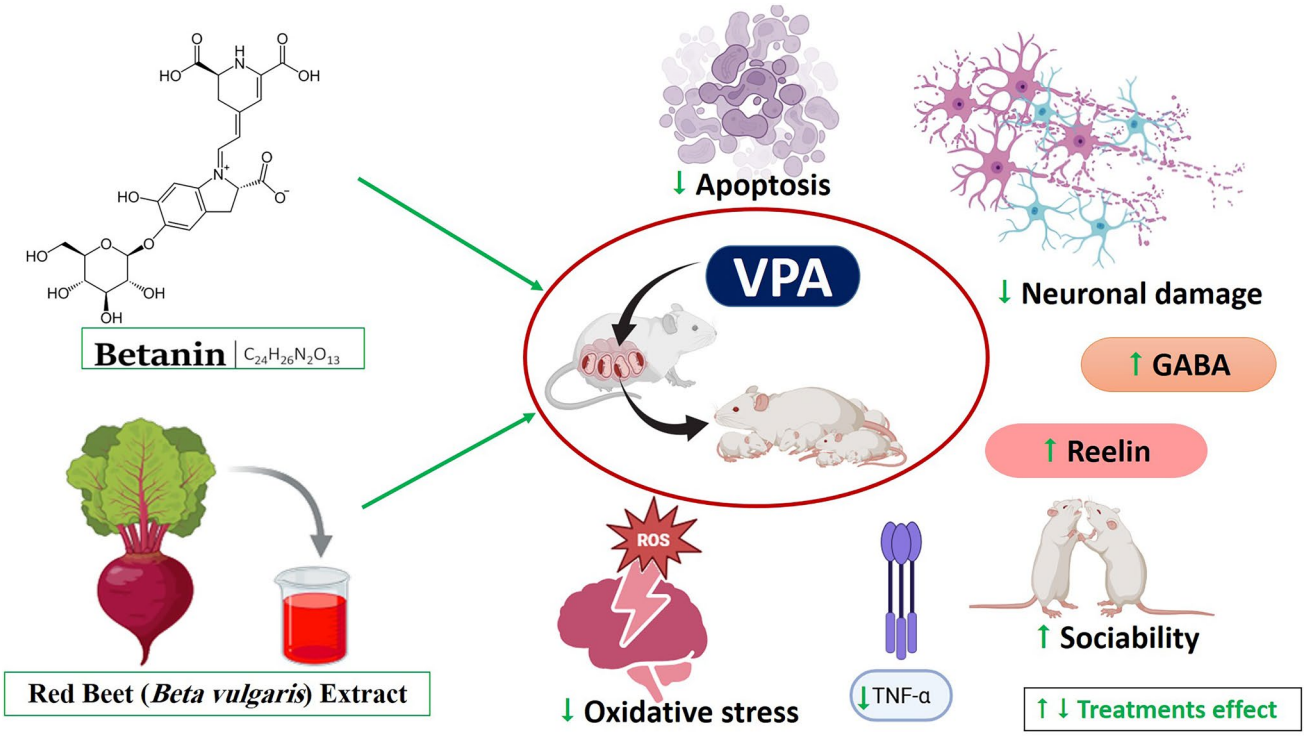
✉ Yasmina M. Abd-Elhakim
yasmina_forensic@hotmail.com

[1] Zoology Department, Faculty of Science, Ain Shams University, Cairo, Egypt

[2] Department of Biological Sciences, Faculty of Science, Galala University, New Galala City 43511, Suez, Egypt

[3] Forensic Medicine and Toxicology Department, Faculty of Veterinary Medicine, Zagazig University, Zagazig 44519, Egypt

Graphical abstract



Keywords *Beta vulgaris* · Betanin · Valproic acid · Oxidative stress · GABA · Reelin

1 Introduction

Autism spectrum disorder (ASD) is a complex neurodevelopmental condition characterized by deficits in social communication and repetitive behaviors, affecting approximately 1% of the global population and presenting lifelong challenges for individuals and families [1, 2]. Males are substantially more likely than females to be diagnosed with ASD, with prevalence ratios ranging from approximately 3:1 to 4:1 across multiple large-scale studies [3, 4]. Although the exact etiology of ASD remains unclear, it is widely accepted that both genetic and environmental factors contribute to its onset [5]. Prenatal exposure to teratogenic agents has been implicated in ASD etiology; in particular, valproic acid (VPA), a widely prescribed anticonvulsant, increases ASD risk when administered during early gestation [6]. In humans, prenatal exposure to VPA has been associated with neural tube defects, including spina bifida, highlighting its potential to disrupt early embryonic development [7]. The VPA-induced rodent model of autism, achieved via a single intraperitoneal injection on embryonic day 12 (E12), recapitulates core behavioral and neuroanatomical hallmarks of ASD, providing construct and clinical validity for preclinical investigations [8]. The most prominent hallmark of ASD is impaired sociability, and animal models of the condition are expected to reflect such deficits [9]. According to a systematic review, prenatal exposure to VPA in rodents induces social behavior abnormalities, particularly evident in the three-chambered social interaction test, the most widely used behavioral assay for evaluating sociability [10].

Offspring exposed to prenatal VPA demonstrate elevated markers of oxidative stress, such as increased lipid peroxidation and diminished antioxidant enzyme activities, alongside heightened neuroinflammatory responses marked by microglial activation and elevated proinflammatory cytokines in key brain regions [11]. These aberrations are thought to contribute to synaptic dysfunction and behavioral phenotypes analogous to those observed in ASD [12]. Prenatal VPA exposure also triggers apoptotic cascades in developing neural circuits, resulting in neuronal loss and altered cortical architecture [13]. Concurrently, it causes dysregulation of synaptic proteins and

signaling molecules, including a reduction in the expression of the extracellular matrix protein Reelin [14]. Reelin, a protein essential for neuronal migration and synaptic plasticity, is typically downregulated in both human ASD cases and in the VPA rodent model [15, 16].

Complementary and alternative therapies based on natural products have garnered increasing interest as adjunctive interventions for ASD, aiming to target the multifactorial pathophysiology of the condition through modulation of oxidative stress, inflammation, and gut–brain interactions [17]. *Beta vulgaris* (red beet) is a nutrient-rich plant widely consumed as food and used in traditional medicine [18]. It is a rich source of bioactive phytochemicals, including betalains (primarily betanin), polyphenols, flavonoids, nitrates, vitamin C, and carotenoids [19]. The plant root and leaves have demonstrated diverse biological activities, including antioxidant, anti-inflammatory, hepatoprotective, antidiabetic, anticancer, and neuroprotective effects [20, 21]. Additionally, ethanolic extracts of beet leaves, rich in polyphenols and betalains, have been shown to improve cognitive function, reduce acetylcholinesterase activity, and attenuate inflammatory cytokine levels in rodent models [22]. Betanin is the major betalain pigment responsible for the deep red color of beetroot. It is a water-soluble compound with a unique structure comprising a chromophore and glycoside moiety, contributing to its stability and biological activity [23]. Betanin has attracted growing attention due to its potent free radical-scavenging properties, high oxygen radical absorbance capacity, and ability to modulate redox signaling pathways [24]. Betanin exhibits potent antioxidant, anti-inflammatory, and antiapoptotic activities [25]. Preclinical studies demonstrate that betanin enhances endogenous antioxidant defenses (e.g., glutathione (GSH), catalase (CAT), and superoxide dismutase (SOD)), mitigates lipid peroxidation, and preserves neuronal integrity in models of cerebral ischemia and neurotoxicity [26].

Extensive evidence supports the safety of both *B. vulgaris* products and their principal pigment, betanin [20, 27]. Acute, subacute, and subchronic rodent studies reveal no adverse effects, even at doses as high as 5 g/kg body weight, while human trials of standardized beetroot extracts (20 g/day over 12 weeks) report excellent tolerability with only minor, unrelated symptoms [28, 29]. Betanin exhibits strong antioxidant and anti-inflammatory actions without evidence of genotoxicity or organ toxicity, and no allergic reactions have been reported in clinical settings [30, 31]. Based on the above pharmacological profile and safety considerations, this study aimed to explore the probable neuroprotective and therapeutic potential of *B. vulgaris*-derived compounds in a well-established model of autism by combining behavioral, biochemical, histological, and molecular approaches. The findings may offer promising insights into the use of plant-based interventions in the management or mitigation of ASD-related impairments.

2 Materials and Methods

2.1 Tested Compounds and Chemicals

Sodium valproate ($C_8H_{15}NaO_2$, molecular weight = 166.19, CAS Number: 1069-66-5, and 98% purity) and betanin (red beet extract diluted with dextrin, $C_{24}H_{26}N_2O_{13}$, molecular weight = 550.47, CAS number: 7659-95-2, and Catalog Number: 901266) were purchased from Sigma-Aldrich Co., supplied by the Egyptian International Center for Imports. Fresh leaves of *B. vulgaris* were sourced from Shibin Al Qanater farms. Upon acquisition, the leaves were subjected to shade drying at ambient room temperature. Once dried, the leaves were powdered finely. The powder was then macerated in 97% ethanol for five days. A solvent-to-plant ratio of 1:20 (w/v) was used during maceration [32]. Then, the mixture was filtered and concentrated to dryness by a rotary evaporator at 40°C. The solvent of the *B. vulgaris* extract was composed of 20 µL of ethanol, 20 µL of Tween 80, 260 µL of normal physiological saline, and 700 µL of water.

2.2 Phytochemical and Antioxidant Evaluation of *B. vulgaris* ethanolic extract

2.2.1 Assessment of Antioxidant Capacity

The antioxidant efficacy of *B. vulgaris* ethanolic extract was evaluated using the DPPH (2, 2-diphenyl-1-picrylhydrazyl) radical scavenging assay, conducted at the Regional Center for Mycology and Biotechnology, Al-Azhar University. A 0.004% DPPH solution was prepared in methanol and stored in the dark at 4°C. The extract was dissolved in methanol, and a small volume was added to the DPPH solution. Absorbance was measured at 515 nm after 16 min using a Milton Roy Spectronic 1201 UV–visible spectrophotometer and continued until a plateau was observed [33]. Ascorbic acid served as the standard antioxidant control [34]. All measurements were performed in triplicate.

2.2.2 Determination of Total Phenolics and Flavonoids of *B. vulgaris* Ethanolic Extract

The total phenolic content of the *B. vulgaris* ethanolic extract was quantified using the Folin–Ciocalteu method [35]. A volume of 5 µL of the extract was mixed with 3 mL of 10% Folin–Ciocalteu reagent and 0.8 mL of 7.5% sodium bicarbonate. The mixture was incubated at room temperature for 30 min. Absorbance was measured at 765 nm using a

Spectronic 1201 spectrophotometer. Results were expressed as milligrams of gallic acid equivalents per gram of extract.

The total flavonoid content of the *B. vulgaris* ethanolic extract was determined based on the method by Chang, Yang [36]. In brief, 0.1 mL of the extract was mixed with 3.9 mL of distilled water and 0.3 mL of 5% sodium nitrite. After 5 min, 0.3 mL of 10% aluminum chloride was added, followed by 2 mL of 1 mM sodium hydroxide after an additional 6 min. The final volume was adjusted with 2.4 mL of distilled water. Absorbance was measured at 510 nm, and flavonoid content was expressed in milligrams of quercetin equivalents per gram of extract.

2.2.3 *HPLC* Analysis of Phenolics, Flavonoids, and Betanin

2.2.3.1 Phenolic Compounds Phenolic profiling was performed using an Agilent 1100 HPLC system with dual LC pumps and a UV/Visible detector. A Hypersil Gold C18 column (250 mm × 4.6 mm, 5 µm) was used. The mobile phase included Solvent A (methanol) and Solvent B (1:25 v/v acetic acid: water). A gradient elution was applied as follows: 0–5 min: 100% Solvent B, 5–15 min: linear increase to 50% Solvent A, 15–25 min: increased to 80% Solvent A, and 25–30 min: returned to 50% Solvent A.

Data were processed using Agilent ChemStation software [37].

2.2.3.2 Flavonoid Compounds Using the same HPLC system and C18 column, flavonoid compounds were analyzed with an isocratic elution of methanol and water (50:50 v/v), adjusted to pH 2.8 with phosphoric acid. The flow rate was maintained at 1.0 mL/min. This method, based on Kuntić, Pejić [38], ensures precise quantification of flavonoids in complex plant matrices.

2.2.3.3 Betanin Content Betanin analysis was also performed on the Agilent 1100 HPLC system equipped with a dual LC pump and UV/Visible light detector. Separation was achieved on a C18 column (4.6 mm × 250 mm, 5 µm particle size, Agilent) with a mobile phase composed of: solvent A: 85% aqueous solution with 1% v/v acetic acid and solvent B: 15% acetonitrile with 1% v/v acetic acid.

The column temperature was maintained at 25 °C, with a flow rate of 1 mL/min. Detection was performed at 540 nm, and results were analyzed using ChemStation software.

2.3 Experimental Animals

This study utilized healthy adult male (180–200 g) and female (150–180 g) Wistar albino rats (*Rattus norvegicus*) obtained from VACSERA (Helwan El-Balad, Cairo Governorate, Egypt). All animals were housed in polyacrylic cages under standardized conditions at the Animal House of the Department of Zoology, Ain Shams University. Rats were grouped with three individuals per cage, and males were housed separately from females. The animal facility maintained a 12-h light/dark cycle, and the temperature and humidity were kept within optimal physiological ranges. The animals were provided ad libitum access to tap water and a standard commercial pellet diet (Extra Animal Food Company, Egypt, Industrial Zone, Inshas, Sharkia), which contained 18.7% protein, 18.82% fiber, 1.64% calcium, and 0.83% phosphorus. All experimental procedures were conducted in compliance with ethical guidelines approved by the Institutional Animal Ethics Committee of Ain Shams University (Approval number ASU-SCI/ZOOL/2025/6/4).

2.4 Breeding Protocol and Gestation Monitoring

For mating, two females identified to be in the estrus phase, determined through vaginal cytology, were paired with one male in each mating cage to optimize conception rates. Female rats were introduced to the males at 6:00 p.m. and remained overnight. Mating success was confirmed the next morning by the presence of sperm in a vaginal smear or the detection of a vaginal plug. The day on which mating was confirmed was designated as gestational day zero (GD0). Pregnant females were then housed individually in separate cages and monitored daily throughout gestation for general health, behavioral changes, and signs of pregnancy progression.

2.5 Experimental Design

Ten pregnant female albino rats were randomly divided into two experimental groups:

- *Control Pregnant Females (n = 5)* Each rat received a single intraperitoneal (i.p.) injection of physiological saline (0.9% NaCl) on embryonic day 12.5 (E12.5).
- *VPA-Treated Pregnant Females (n = 5)* Each rat received a single i.p. injection of VPA at a dose of 400 mg/kg body weight, dissolved in 0.9% physiological saline, also on E12.5 [39]. This dose was selected based on previous research investigating the effects of moderate doses [40–42]. These studies aimed to minimize toxicity and reabsorption, which were noted at higher doses, such as 500 and 600 mg/kg, particularly in female rats [43]. Moreover, this dosage has been shown to induce behavioral and neurobiological changes in offspring that closely resemble those observed in individuals with autism, including deficits in sociability, repetitive behaviors, and altered empathy-like responses [44].

Postnatal day 1 (PND 1) was defined as the day of birth, and only male offspring were selected for further

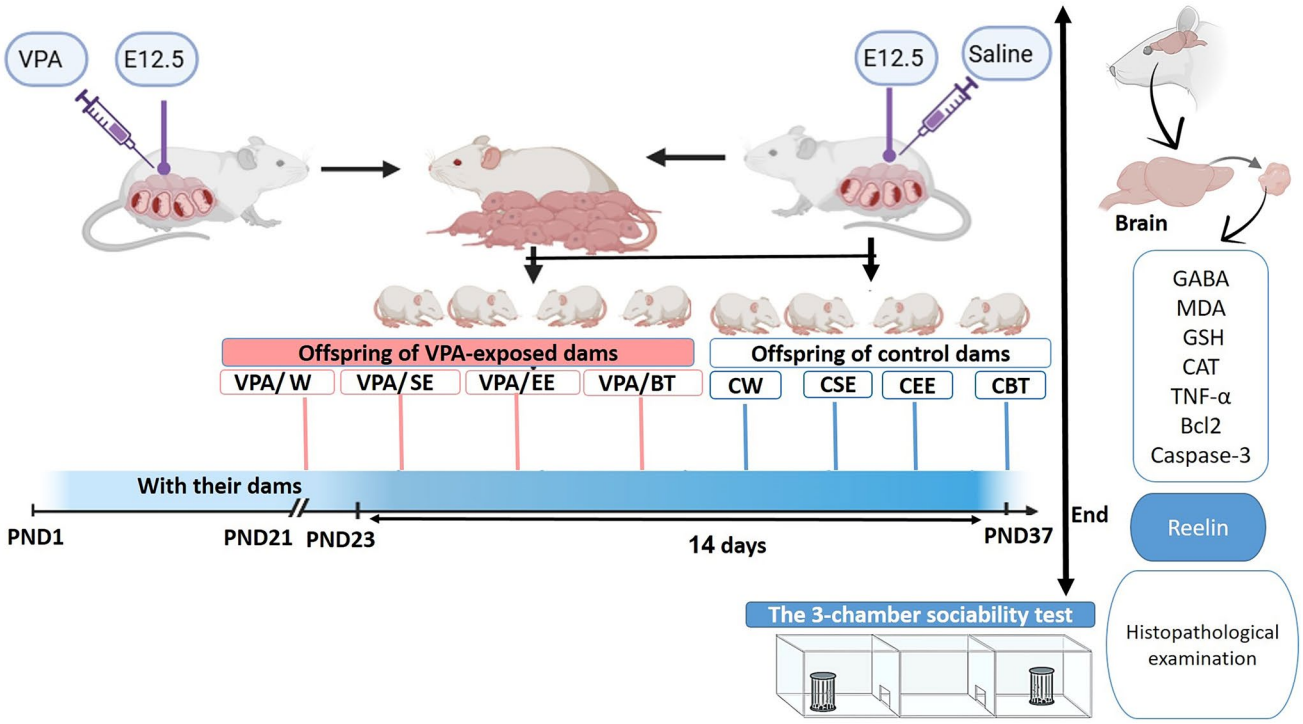


Fig. 1 Experimental design and timeline of prenatal valproic acid (VPA) exposure and postnatal treatments in rat offspring. Pregnant dams were injected intraperitoneally with either VPA (a single i.p. injection of 400 mg/kg body weight) or physiological saline at embryonic day 12.5 (E12.5). Offspring from VPA-exposed and control (saline-treated) dams were reared with their mothers until postnatal day 21 (PND21). From PND23 to PND37, male pups offspring were allocated to eight groups ($n = 6$ per group) according to prenatal exposure and postnatal treatment: distilled water (CW and VPA/CW groups), ethanolic extract solvent (CSE and VPA/SE groups), *Beta vulgaris* leaf ethanolic extract (CEE and VPA/EE groups; 200 mg/kg), or betanin (CBT and VPA/BT groups; 25 mg/kg). On PND37, animals underwent the three-chamber sociability test, followed by biochemical analyses of gamma-aminobutyric acid (GABA), malondialdehyde (MDA), reduced glutathione (GSH), catalase (CAT), tumor necrosis factor-alpha (TNF-α), B-cell lymphoma 2 (Bcl-2), and caspase-3, as well as evaluation of Reelin expression and histopathological examination of brain tissues

experimentation. The dams were permitted to care for their litters naturally until weaning on PND 21. On PND 23, the pups were weaned and randomly assigned into eight experimental groups (n = 6 per group) based on their respective prenatal exposures and the designated postnatal interventions. These interventions started on PND 23 and continued for 14 consecutive days, as outlined in Fig. 1 and detailed below:

Control Groups (Offspring of Control Non-VPA-exposed Dams):

- *Control Group I (CW)* orally administered distilled water.
- *Control Group II (CSE)* orally administered 1mL of the ethanolic extract solvent.
- *Control Group III (CEE)* orally administered 200 mg/kg of ethanolic *B. vulgaris* leaf extract (dissolved in 1 mL solvent) [45].
- *Control Group IV (CBT)* orally administered 25 mg/kg of betanin (dissolved in 1 mL distilled water) [46].

VPA-exposed Groups (Offspring of VPA-Exposed Dams):

- *Group V (VPA/W)* orally administered distilled water.
- *Group VI (VPA/SE)* orally administered 1 mL of the ethanolic extract solvent.
- *Group VII (VPA/EE)* orally administered 200 mg/kg of ethanolic *B. vulgaris* leaf extract (dissolved in 1 mL solvent).
- *Group VIII (VPA/BT)* orally administered 25 mg/kg of betanin (dissolved in 1 mL distilled water).

2.6 Behavioral Analysis

Behavioral testing was conducted on PND 37, immediately following the completion of 14 days of treatment (PND 23– PND 37). Before testing, offspring were briefly isolated for 30 min in a clean holding cage to minimize social carryover effects. Behavioral studies included the three-chamber sociability test, assessing social preference and social novelty, using a protocol adapted from Kim, Kim [47] and modified by Bambini-Junior, Zanatta [48]. The apparatus

was constructed of clear acrylic, measuring 60 cm × 45 cm × 45 cm, with three interconnected chambers. Wire cages in the side chambers held a 'novel rat' or 'novel object' for testing sociability. The procedure involved three phases: (1) Habituation, allowing the test rat free movement for 5 min; (2) Sociability, where a novel rat was introduced, and time spent with the novel rat vs. novel object was recorded; the sociability index (SI) was computed from the interactions. (3) Social novelty, introducing a second novel rat to evaluate preference between the known rat (novel rat 1 in the sociability stage) and the unknown rat (novel rat 2). The apparatus was cleaned with 70% ethanol after each trial to avoid olfactory bias. The social novelty preference index (SNI) was computed from the interactions. Chambers were sanitized with 70% alcohol between tests to prevent scent bias.

Calculations

$$(\mathrm{SI}) = \frac{\text{time exploring novel rat 1} - \text{time exploring novel object}}{\text{time exploring novel rat 1} + \text{time exploring novel object}}$$

$$\mathrm{SNI} = \frac{\text{time exploring novel rat 2} - \text{time exploring known rat}}{\text{time exploring novel rat 2} + \text{time exploring known rat}}$$

2.7 Brain Tissue Collection and Preparation

After completion of the behavioral tests, rats were euthanized by decapitation under anesthesia (100 mg/kg pentobarbital sodium, intraperitoneally). Each brain was carefully removed and bisected along the mid-sagittal plane to obtain the right and left hemispheres. The right hemisphere was fixed in 10% neutral-buffered formalin for 24 h for histopathological evaluation, while the left hemisphere was used for molecular and biochemical analyses. From the left hemisphere, the cerebral cortex was dissected on an ice-cold surface, immediately snap-frozen in liquid nitrogen, and stored at − 80 °C for biochemical assays and gene expression analysis.

2.8 Biochemical and Neurochemical Assays

2.8.1 Preparation of Tissue Homogenate

For colorimetric assays (MDA, GSH, and CAT): Brain samples were perfused with phosphate-buffered saline (PBS, pH 7.4) enriched with 0.16 mg/mL heparin to eliminate red blood cells and clots. Tissues were then homogenized using a PRO 250 homogenizer in a cold buffer containing 50 mM potassium phosphate (pH 7.5) with 1 mM EDTA, at a ratio of 5–10 mL buffer per gram of tissue. Homogenates were centrifuged at 4,000 rpm for 15 min at 4°C. The supernatants were stored at −80°C until analysis.

For ELISA Assays (TNF-α, Bcl2, Caspase-3, and GABA): Tissues were rinsed with ice-cold PBS, minced, and homogenized in fresh lysis buffer (volume-to-weight ratio 1:20 to 1:50) using a glass homogenizer. Samples were then sonicated until clear and centrifuged at 10,000 × g for 5 min. The resulting supernatants were used immediately for ELISA.

2.8.2 Gamma-Aminobutyric Acid (GABA) Determination

GABA levels were quantified using a rat GABA ELISA Kit (MyBioSource, San Diego, California, USA, Catalog no. MBS269152, sensitivity: 12 pg/mL, and detection range: 31.2–2,000 pg/mL). Samples were bound to pre-coated antibodies, followed by the addition of biotinylated antibodies, avidin-peroxidase conjugate, and substrate. The color reaction was stopped, and absorbance was measured at 450 nm. Concentrations were calculated based on a standard curve.

2.8.3 Reduced Glutathione (GSH) Determination

GSH levels were determined colorimetrically [49]. After adding 0.5 mL of trichloroacetic acid to the homogenate and incubating at room temperature for 5 min, samples were centrifuged at 3,000 rpm for 15 min. From the supernatant, 0.5 mL was mixed with 1.0 mL phosphate buffer and 0.1 mL of 5, 5'-dithiobis (2-nitrobenzoic acid). Absorbance was measured at 405 nm after 5–10 min.

2.8.4 Catalase Activity Assay

Using Aebi [50] method, 0.05 mL of homogenate was added to assay cuvettes along with phosphate buffer (pH 7.0). After 1-min incubation at 25 °C, chromogen-inhibitor solution (0.2 mL) and peroxidase-aminoantipyrine (0.5 mL) were added. Following a 10-min incubation at 37 °C, absorbance was measured at 510 nm.

2.8.5 Malondialdehyde (MDA) Determination

MDA levels were assessed based on Ohkawa, Ohishi [51]. A 0.2 mL sample was mixed with 1.0 mL chromogen (thiobarbituric acid, detergent, stabilizer) and heated in boiling water for 30 min. After cooling, absorbance was measured at 534 nm. The color remained stable for at least 6 h.

2.8.6 Tumor Necrosis Factor Alpha (TNF-α) and B-Cell Leukemia/Lymphoma 2 (Bcl2) Determination

TNF-α was measured using an ELISA kit (Cloud-Clone Corp., Katy, Texas, USA, Catalog no. SEA133Ra,

sensitivity: 5.9 pg/mL, and detection range: 15.6–1,000 pg/mL). Standards and samples (100 µL) were incubated at 37 °C for 1 h. After washing, 100 µL each of detection reagents A and B was added sequentially with incubations and washes. Finally, 90 µL TMB substrate was added and incubated in the dark, followed by 50 µL stop solution. Absorbance was read at 450 nm.

Using a rat Bcl2 ELISA Kit (Cloud-Clone Corp., Katy, Texas, USA, Catalog no. SEA778Ra, sensitivity: 33 pg/mL, and detection range: 78–5,000 pg/mL), a sandwich immunoassay was performed. 100 µL of samples and standards were incubated for 1 h at 37 °C. Detection reagents were applied sequentially with intermediate washes. TMB substrate facilitated a colorimetric reaction, stopped with sulfuric acid, and the absorbance was recorded at 450 nm.

2.8.7 Caspase-3 Determination

Caspase-3 levels were measured with a rat CASP3 ELISA Kit (Cloud-Clone Corp., Katy, Texas, USA, Catalog no. SEA626Ra, sensitivity: 0.060 ng/mL, and detection range: 0.156–10 ng/mL). Samples and standards (100 µL) were incubated for 1 h at 37 °C. Detection reagents, including HRP, were applied with appropriate washes. TMB substrate induced a color change, halted by the stop solution, and the optical density was recorded at 450 nm.

2.9 Gene expression Analysis by SYBR Green Real-time PCR

Total RNA was extracted from brain tissue samples using the RNeasy Mini Kit (Qiagen, Cat. No. 74104), following the manufacturer's protocol. Briefly, 30 mg of each brain region was weighed and transferred into sterile 2 ml screw-capped tubes containing sterile glass beads. To each tube, 600 µl of Buffer RLT supplemented with 10 µl/ml β-mercaptoethanol (Sigma-Aldrich) was added. Samples were homogenized using a TissueLyser (Qiagen) at 30 Hz for 2 min. The lysates were then centrifuged at 14,000 rpm for 3 min. The resulting supernatants were mixed with an equal volume of 70% ethanol (prepared from 96% ethanol, Applichem) and transferred to RNeasy spin columns placed in 2 ml collection tubes. After centrifugation at 14,000 rpm for 1 min, the flow-through was discarded, and the process was repeated for the remaining sample volume. RNA purification was continued by washing the columns with 700 µl of Buffer RW1, followed by two washes with 500 µl Buffer RPE, the second of which included a 2-min centrifugation. Total RNA was eluted with 50 µl RNase-free water and quantified before storage at − 80 °C until further use.

For real-time PCR analysis, complementary DNA (cDNA) was synthesized using RevertAid Reverse Transcriptase (Thermo Fisher, Cat. No. EP0441). The PCR reactions were prepared using the QuantiTect SYBR Green PCR Kit (Qiagen, Cat. No. 204141) in a final volume of 25 µl per reaction. Each reaction contained 12.5 µl of 2 × QuantiTect SYBR Green PCR Master Mix, 0.25 µl reverse transcriptase, 0.5 µl each of forward and reverse primers (20 pmol; Metabion, Germany), 8.25 µl RNase-free water, and 3 µl of RNA template. The oligonucleotide sequences for target genes were as follows: for ß-actin (reference gene), forward 5'-TCCTCCTGAGCGCAAGTACTCT-3' and reverse 5'-GCTCAGTAACAGTCCGCCTAGAA-3' [52]; for Reelin, forward 5'-AAACTACAGCGGGTGGAACC-3' and reverse 5'-ATTTGAGGCATGACGGACCTATAT-3' [53]. Real-time PCR amplification was carried out using a Stratagene MX3005P system. Cycling conditions were as follows: reverse transcription at 50 °C for 30 min, followed by an initial denaturation at 94 °C for 15 min. This was followed by 40 amplification cycles consisting of 94 °C for 15 s, annealing at 60 °C (for ß-actin) or 55 °C (for Reelin) for 30 s with optics on, and extension at 72 °C for 30 s. A dissociation curve was generated after amplification with the following settings: 94 °C for 1 min, 60 °C (ß-actin) or 55 °C (Reelin) for 1 min, and a final denaturation at 94 °C for 1 min.

Amplification curves and threshold cycle (Ct) values were analyzed using the Stratagene MX3005P software. Gene expression levels were quantified using the comparative Ct (ΔΔCt) method, as described by Livak and Schmittgen [54]. Relative expression was calculated using the formula 2^(-ΔΔCt), where ΔΔCt = ΔCt_reference – ΔCt_target, with ΔCt_target = Ct_control – Ct_treatment and ΔCt_reference = Ct_control – Ct_treatment. β-actin was used as the internal reference gene for normalization across samples.

2.10 Histopathological Examination

Rat brain tissues were extracted and immediately fixed in 10% neutral buffered formalin for 24 to 48 h to adequately preserve tissue morphology and prevent autolysis and decomposition. Following fixation, the tissues underwent sequential dehydration through a graded ethanol series (70%, 80%, 95%, and 100%), cleared in xylene, and embedded in paraffin wax. Paraffin-embedded tissues were sectioned into 5 µm-thick slices using a microtome and mounted onto glass slides in preparation for histological staining. This method ensures preservation of structural integrity and histological detail, enabling reliable microscopic examination [55]. The tissue sections were deparaffinized in xylene and rehydrated through a descending alcohol series, ending in distilled water. Sections were then stained with Hematoxylin for eight minutes to visualize cell nuclei, followed by rinsing in tap water and brief differentiation in 1% acid alcohol. After a second rinse in water, the sections were counterstained with Eosin for three minutes, which highlights cytoplasmic

components and the extracellular matrix in varying shades of pink. Following staining, the slides were dehydrated again through ascending alcohol concentrations, cleared in xylene, and mounted using a resinous medium for long-term preservation and examination.

The lesion score was conducted in different brain regions, the cerebral cortex, hippocampus, and cerebellum. A score ranging from 0 to 3 was given to describe the degree of neuronal degeneration in the different brain regions, where 0 = no degeneration, 1 = few degenerating cells, 2 = moderate neuronal degeneration, and 3 = diffuse neuronal degeneration, and the mean degeneration score was calculated in each group.

2.11 Statistical Analysis

To ensure that the data met the assumptions of normality and homogeneity of variances, the Kolmogorov–Smirnov and Levene's tests were conducted before analysis of variance (ANOVA). When assumptions were met, one-way ANOVA was applied to compare group means, followed by Tukey's post hoc test to identify significant differences between treatment groups. Histopathological scoring data were analyzed using the Kruskal–Wallis test, followed by Dunn's post hoc multiple-comparison test. Results are presented as mean ± standard error (SE), and statistical significance was considered at $p < 0.05$. Statistical analyses were performed using GraphPad Prism (version 8).

3 Results

3.1 Optimization and Characterization of the Ethanolic Extract of *B. vulgaris* Leaves

3.1.1 Antioxidant Activity of *B. vulgaris* Extract

The extract demonstrated a concentration-dependent scavenging effect, as shown in Fig. 2. At the highest concentration (1280 µg/mL), the extract achieved 92.68% inhibition, whereas lower concentrations showed a gradual decline in activity, reaching 2.08% at 2.5 µg/mL and 0% at 0 µg/mL. The IC_{50} value was calculated to be 125.53 ± 2.31 µg/mL, indicating moderate antioxidant potential when compared with the ascorbic acid reference standard (IC_{50} = 10.62 ± 0.84 µg/mL).

3.1.2 Total phenolic and Flavonoid Contents

Quantitative analysis revealed that the total phenolic content in the extract was 76.02 ± 4.66 mg/g, while the total flavonoid content was 49.78 ± 3.14 mg/g. These high concentrations suggest a rich presence of bioactive phytochemicals with potential antioxidant properties.

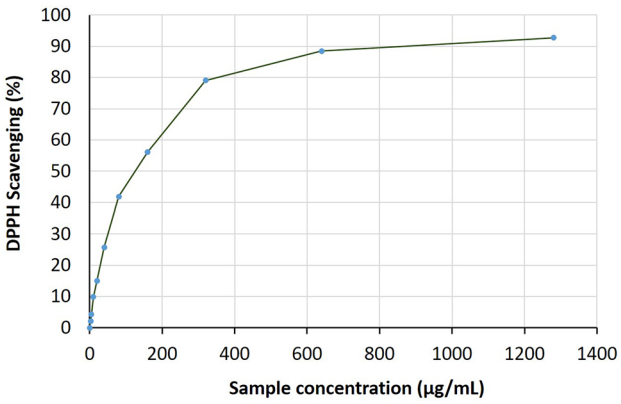


Fig. 2 The DPPH scavenging activity curve for the ethanolic extract of *Beta vulgaris* leaves

3.1.3 HPLC Analysis of Phenolic and Flavonoid Compounds and Betanin

HPLC analysis identified and quantified several key phenolic compounds in the extract (Fig. 3A). Among them, p-coumaric acid was the most abundant (22.14 µg/g), followed by gallic acid (20.63 µg/g), cinnamic acid (16.51 µg/g), and catechol (9.66 µg/g). As shown in Fig. 3B, HPLC profiling also identified a range of flavonoids. Apigenin was found in the highest concentration (7.06 µg/g), followed by 7-OH flavone (5.88 µg/g), myricetin (3.14 µg/g), quercetin (2.06 µg/g), and catechin (2.01 µg/g). The content of betanin, a major bioactive pigment in *B. vulgaris*, was analyzed separately and quantified at 18.26 mg/g, with a retention time of 6.1 min (Fig. 3C).

3.2 Gross Morphological Abnormalities in VPA-treated Neonatal Rats

Visual examination of neonatal rats revealed distinct morphological differences between control and VPA-treated groups, as shown in Fig. 4. Control pups (Fig. 4A) exhibited normal body posture and tail morphology, with no visible abnormalities. In contrast, pups prenatally exposed to VPA displayed several gross developmental malformations. These included pronounced tail deformities such as kinking, bending, and nodular protrusions (Figs. 4B–D, yellow arrows). Curvature of the posterior spine and abnormal alignment of the caudal region were also observed (Fig. 4E), suggesting disruptions in axial skeletal development. These malformations were consistently observed among VPA-exposed litters and were absent in the control group, indicating a teratogenic

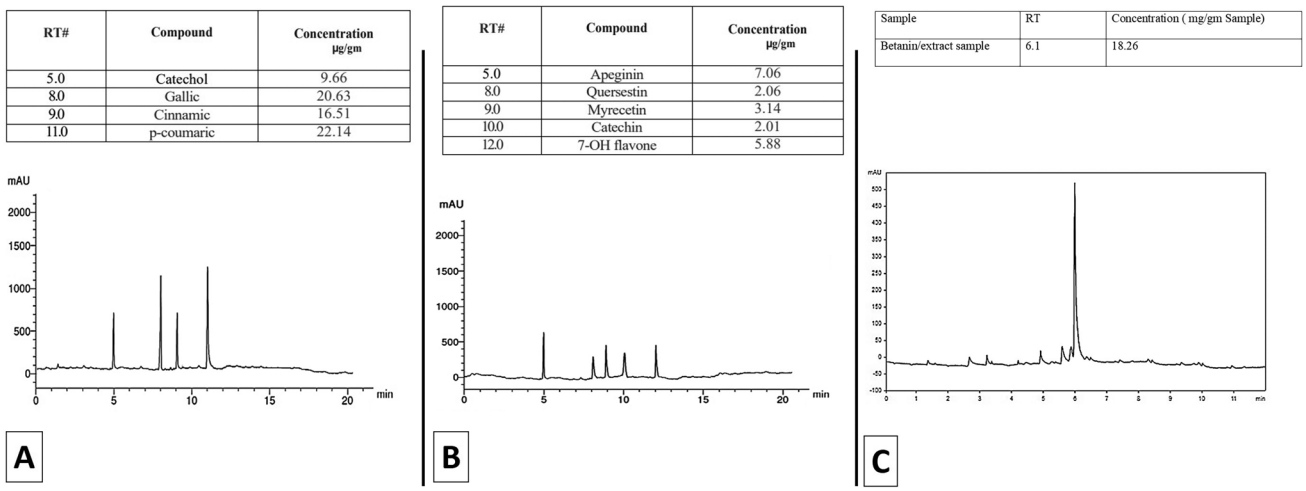


Fig. 3 HPLC chromatographic analysis of phenolic and flavonoid compounds in red beet ethanolic extract and betanin. (A) Phenolic content in red beet extract with identified compounds: Catechol (5.0 min), Gallic acid (8.0 min), Cinnamic acid (9.0 min), and p-Coumaric acid (11.0 min). (B) Flavonoid content in red beet extract showing Apigenin (5.0 min), Quercetin (8.0 min), Myricetin (9.0 min), Catechin (10.0 min), and 7-OH flavone (12.0 min). (C) Betanin chromatogram detected at 6.1 min with a concentration of 18.26 mg/g in the sample

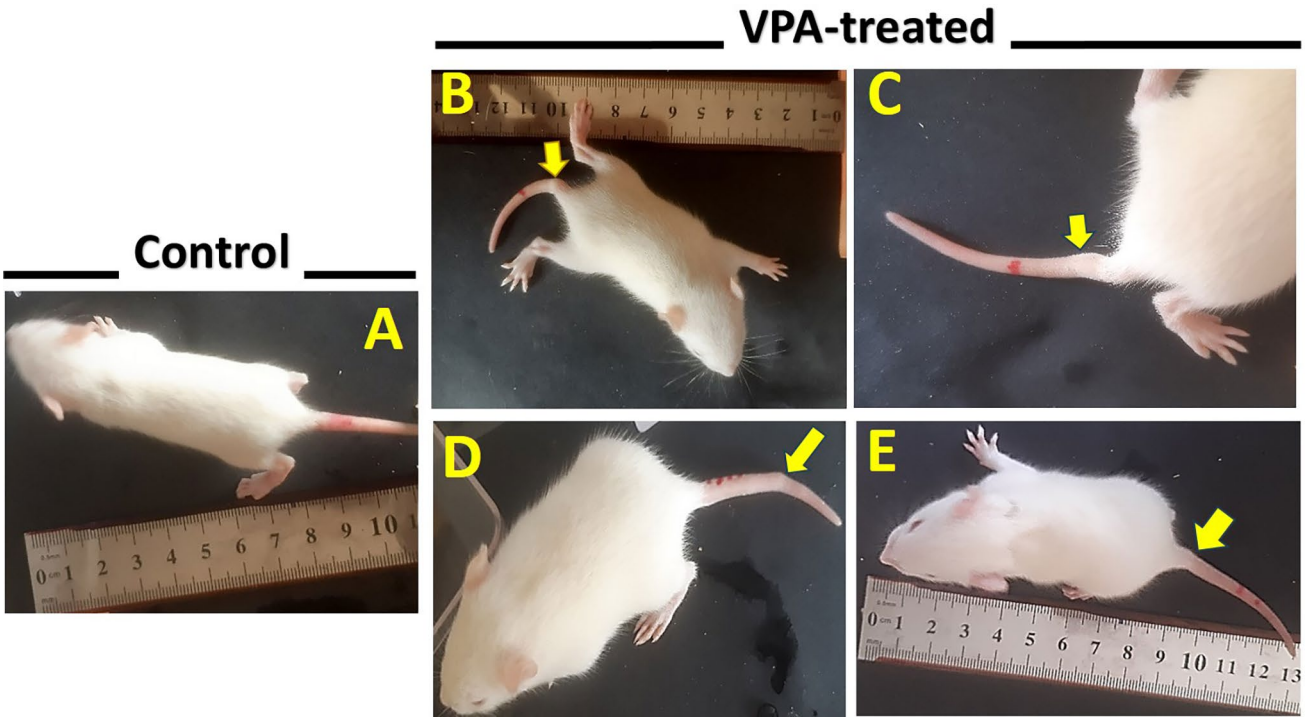


Fig. 4 Representative photos of the external phenotypic differences between control (A) and valproic acid (VPA)-treated (B–E) neonatal rats, focusing on tail morphology and overall body development. A (Control): A representative control rat shows normal tail morphology and body development with no visible deformities. B–E (VPA-Treated): Neonatal rats exposed to VPA exhibit several gross morphological abnormalities: B: A distinct kink or bending at the base of the tail (yellow arrow). C: view of tail malformation, highlighting a marked curvature (yellow arrow). D: Additional tail deformity, including a series of small nodules or kinks along the tail (yellow arrow). E: Aberrant curvature of the posterior spine and tail region (yellow arrow)

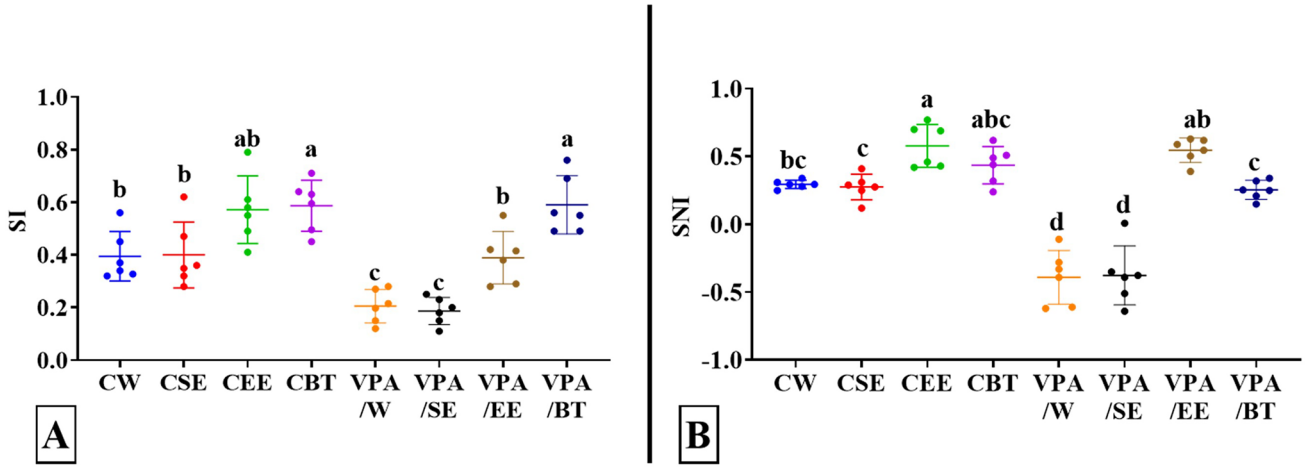


Fig. 5 Behavioral assessment of sociability and social novelty preference in prenatally valproic acid (VPA)-exposed offspring and treatment groups. (A) Sociability Index (SI) and (B) Social Novelty Index (SNI) across experimental groups: control water (CW), control betanin (CBT), control solvent extract (CSE), control ethanolic extract (CEE), prenatally VPA-exposed and postnatally water-treated (VPA/W), prenatally VPA-exposed and postnatally solvent extract-treated (VPA/SE), prenatally VPA-exposed and postnatally ethanolic extract-treated (VPA/EE), and prenatally VPA-exposed and postnatally betanin-treated (VPA/BT). Data are presented as mean ± SE ($n = 6$ per group). [a, b, c, and d] columns with different superscripts are statistically different at $P < 0.05$

effect of VPA on caudal vertebral and tail formation during embryonic development.

3.3 Betanin Restored Sociability and Social Novelty Preference Impaired by Prenatal-VPA Exposure

The effects of various treatments on SI and SNI in male rat pups are presented in Fig. 5. All control groups (CW, CBT, CSE, and CEE) maintained stable and positive SI and SNI values, with no significant differences among them, and consistently outperformed the VPA/W group. In contrast, the VPA/W group exhibited significant impairments in both sociability and social novelty behavior, as evidenced by a markedly reduced SI ($p < 0.05$ vs. CW) and a strongly negative SNI ($p < 0.0001$ vs. CW). The VPA/SE group displayed no significant improvement compared to VPA/W. Conversely, both VPA/EE and VPA/BT treatments significantly ameliorated these impairments. VPA/EE rats showed a notable increase in SI ($p < 0.01$ vs. VPA/W) and a significant recovery in SNI ($p < 0.0001$ vs. VPA/W). Besides, VPA/BT exhibited a significant increase in SI ($p < 0.0001$ vs. VPA/W) and SNI ($p < 0.0001$ vs. VPA/W). A significant ($p < 0.05$) difference was observed between VPA/EE and VPA/BT in SI and SNI.

3.4 Effect of Treatments on Cortical GABA Levels

As illustrated in Fig. 6, the concentration of GABA was significantly altered among the experimental groups. The VPA/W group exhibited a significant reduction in GABA levels compared to all control groups (CW, CSE, CEE, and

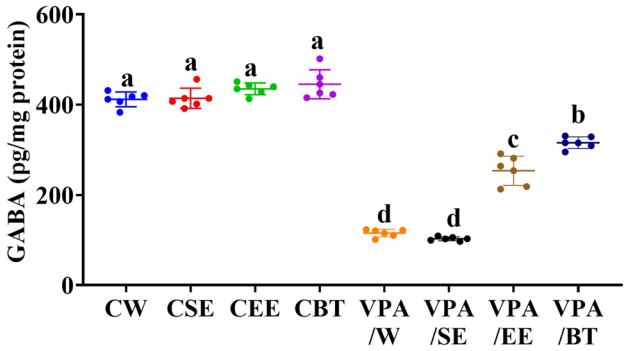


Fig. 6 Gamma-aminobutyric acid (GABA) content in brain tissue of prenatally valproic acid (VPA)-exposed offspring and treatment groups. (A) GABA levels across experimental groups: control water (CW), control betanin (CBT), control solvent extract (CSE), control ethanolic extract (CEE), prenatally VPA-exposed and postnatally water-treated (VPA/W), prenatally VPA-exposed and postnatally solvent extract-treated (VPA/SE), prenatally VPA-exposed and postnatally ethanolic extract-treated (VPA/EE), and prenatally VPA-exposed and postnatally betanin-treated (VPA/BT). Data are expressed as mean ± SE ($n = 6$). [a, b, c, and d] columns with different superscripts are statistically different at $P < 0.05$

CBT) ($p < 0.0001$). Among the treatment groups, VPA/BT and VPA/EE significantly elevated GABA levels relative to the VPA/W group ($p < 0.0001$). Importantly, VPA/BT treatment restored GABA levels to near-control values and demonstrated greater efficacy than VPA/EE, as evidenced by the significant difference between the two ($p < 0.001$). The VPA/SE group showed no considerable improvement in GABA levels compared to VPA/W. The control groups maintained

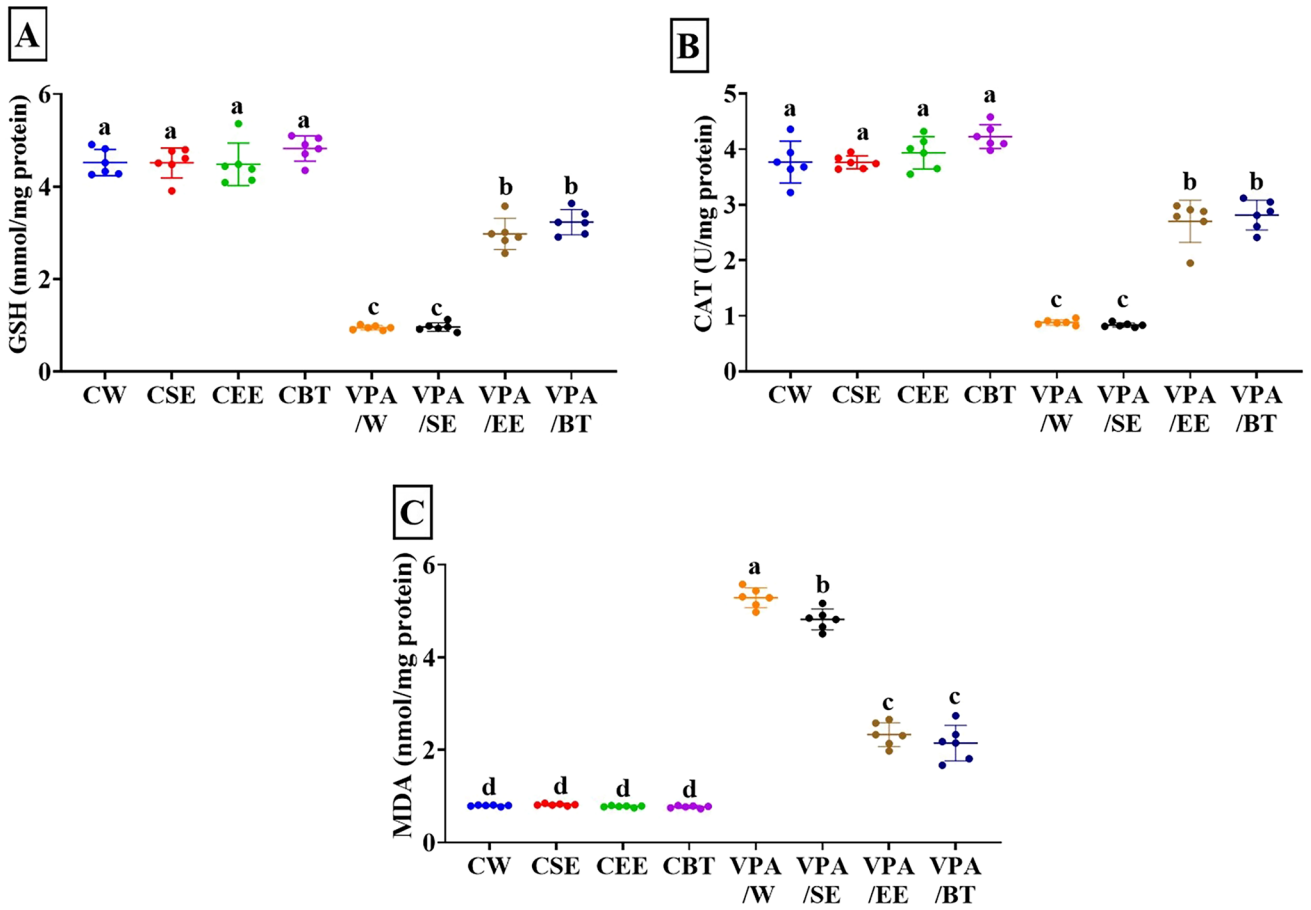


Fig. 7 Oxidative stress biomarkers in brain tissue of control and prenatally valproic acid (VPA)–exposed offspring. (A) Reduced glutathione (GSH) levels, (B) catalase (CAT) activity, and (C) malondialdehyde (MDA) levels across experimental groups: control water (CW), control betanin (CBT), control solvent extract (CSE), control ethanolic extract (CEE), prenatally VPA-exposed and postnatally water-treated (VPA/W), prenatally VPA-exposed and postnatally solvent extract-treated (VPA/SE), prenatally VPA-exposed and postnatally ethanolic extract-treated (VPA/EE), and prenatally VPA-exposed and postnatally betanin-treated (VPA/BT). Data are expressed as mean ± SE ($n = 6$). [a, b, and c] columns with different superscripts are statistically different at $P < 0.05$

consistently high and comparable GABA levels, with no significant differences observed among them ($p > 0.05$).

3.5 Effects on Oxidative Stress Markers

The impact of various treatments on oxidative stress and antioxidant defense mechanisms was evaluated by measuring levels of GSH, MDA, and CAT in the cerebral cortex of male rat pups, as presented in Fig. 7. The VPA/W group exhibited pronounced oxidative stress, characterized by a significant decrease in GSH and CAT levels ($p < 0.0001$) and a significant elevation in MDA levels ($p < 0.001$) compared to the control groups (CW, CSE, CEE, and CBT). Similarly, the VPA/SE group showed persistent oxidative imbalance with significantly reduced antioxidant markers and elevated lipid peroxidation compared to controls. In contrast, both the VPA/EE and VPA/BT groups demonstrated significant restoration of GSH and CAT levels ($p < 0.0001$) and marked reductions in MDA concentrations ($p < 0.0001$) relative to the VPA/W group. No significant difference was detected between VPA/EE and VPA/BT in any of the oxidative parameters. Moreover, no significant variations were observed among the control groups across all oxidative and antioxidant markers ($p > 0.05$).

3.6 Effects on the Pro-inflammatory Cytokine, TNF-α, Brain Levels

The concentration of TNF-α was measured in the cerebral cortex of male rat pups across the different experimental groups, as illustrated in Fig. 8. The VPA/W group showed a significant elevation in TNF-α levels compared to all control groups (CW, CBT, CSE, and CEE; $p < 0.0001$). Yet, treatment with both VPA/BT and VPA/EE markedly reduced TNF-α levels relative to the VPA/W group ($p < 0.0001$).

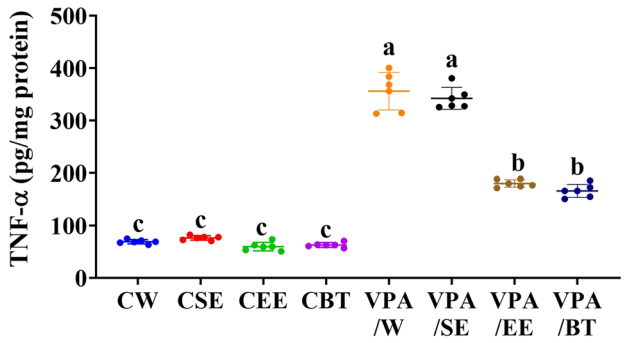


Fig. 8 Tumor necrosis factor-alpha (TNF-α) content in brain tissue of prenatally valproic acid (VPA)-exposed offspring and treatment groups. (A) TNF-α levels across experimental groups: control water (CW), control betanin (CBT), control solvent extract (CSE), control ethanolic extract (CEE), prenatally VPA-exposed and postnatally water-treated (VPA/W), prenatally VPA-exposed and postnatally solvent extract-treated (VPA/SE), prenatally VPA-exposed and postnatally ethanolic extract-treated (VPA/EE), and prenatally VPA-exposed and postnatally betanin-treated (VPA/BT). Data are expressed as mean ± SE ($n = 6$). [a, b, and c] columns with different superscripts are statistically different at $P < 0.05$

However, there was no significant difference between VPA/BT and VPA/EE in terms of TNF-α suppression ($p > 0.05$). The control groups maintained consistently low levels of TNF-α, with no significant differences observed among them ($p > 0.05$).

3.7 Effect on Apoptotic Markers

The levels of BCL2 (anti-apoptotic) and Caspase-3 (pro-apoptotic) were measured in the cerebral cortex of male rat pups to assess apoptotic activity across experimental groups, as shown in Fig. 9. The VPA/W group exhibited a significant decrease in BCL2 levels and a marked increase in Caspase-3 levels compared to all control groups (CW, CSE, CEE, and CBT; $p < 0.0001$ for both). Treatment with VPA/BT and VPA/EE significantly restored BCL2 expression ($p < 0.0001$ and $p < 0.001$, respectively) and attenuated Caspase-3 levels ($p < 0.0001$). No significant differences were observed between VPA/BT and VPA/EE for either marker ($p > 0.05$). The control groups showed stable, high BCL2 and low Caspase-3 levels, with no significant variations among them ($p > 0.05$).

3.8 Histological Findings

Microscopic examination of brain sections from the control groups (CW, CSE, CEE, and CBT) revealed normal histological architecture across the cerebral cortex, hippocampus, and cerebellum, with no detectable pathological alterations (Figs. 10, 11, and 13). In contrast, brain sections from the VPA/W group exhibited severe histopathological changes in all examined brain regions. The cerebral cortex showed numerous dark, shrunken neurons accompanied by neuronophagia, indicating substantial neuronal damage (Fig. 10 I and J). Figure 12 (A-F) showed the hippocampus to be markedly affected, with a widespread presence of dark neurons across the CA1, CA2, CA3, CA4, and dentate gyrus regions, along with pronounced neuronal loss.

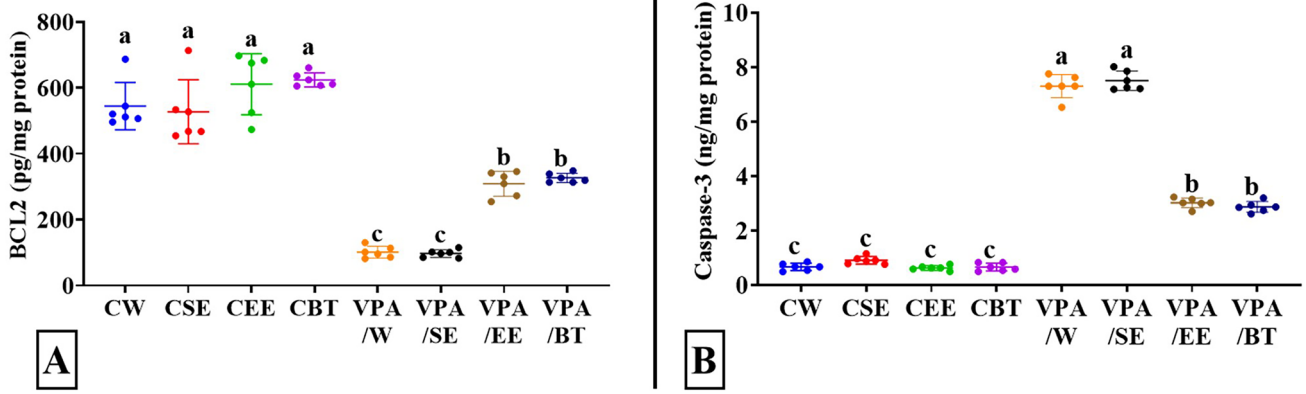


Fig. 9 Apoptosis biomarkers in brain tissue of control and prenatally valproic acid (VPA)-exposed offspring. (A) BCL-2 and (B) Caspase-3 levels across experimental groups: control water (CW), control betanin (CBT), control solvent extract (CSE), control ethanolic extract (CEE), prenatally VPA-exposed and postnatally water-treated (VPA/W), prenatally VPA-exposed and postnatally solvent extract-treated (VPA/SE), prenatally VPA-exposed and postnatally ethanolic extract-treated (VPA/EE), and prenatally VPA-exposed and postnatally betanin-treated (VPA/BT). Data are expressed as mean ± SE ($n = 6$). [a, b, and c] columns with different superscripts are statistically different at $P < 0.05$

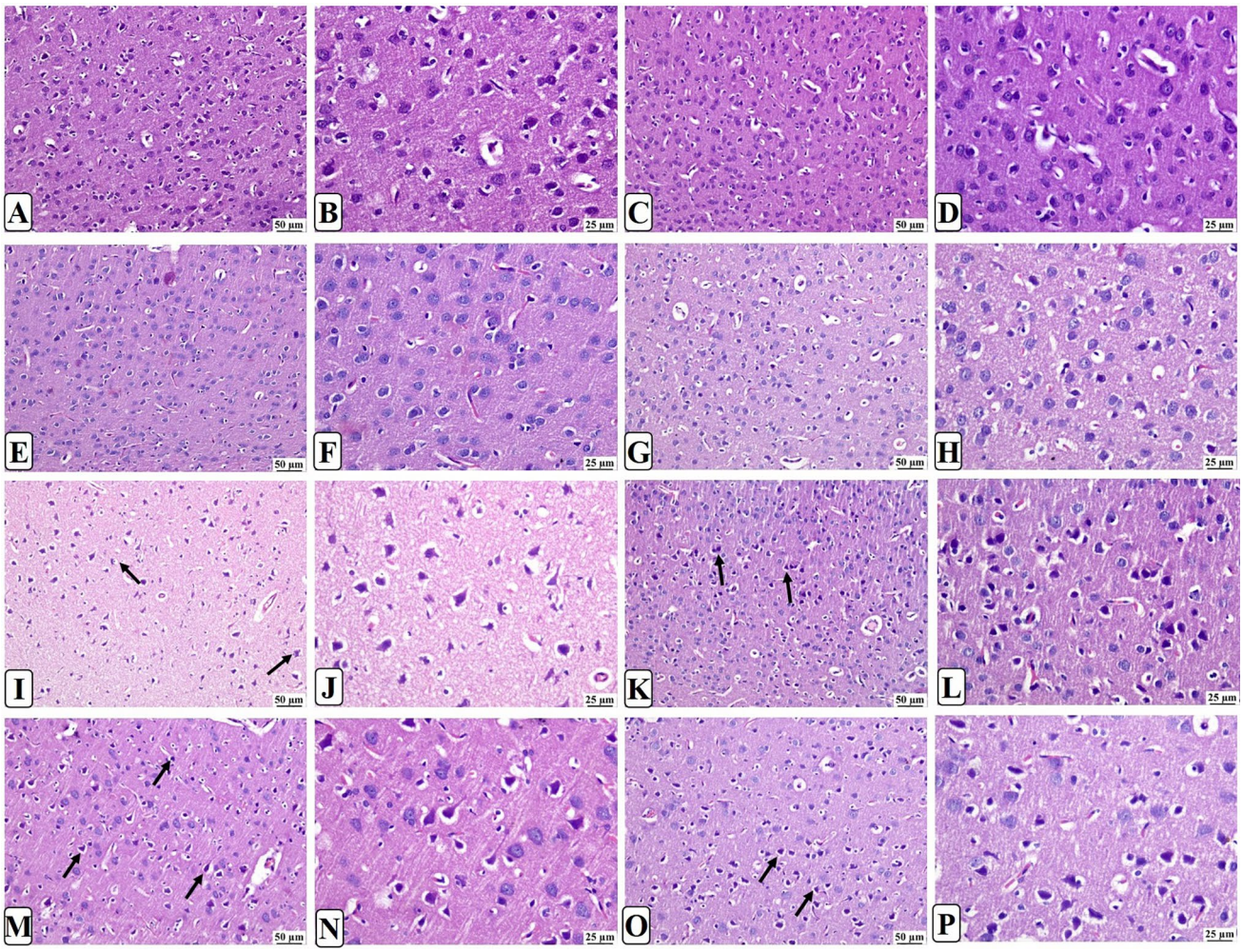


Fig. 10 Representative photomicrographs of the cerebral cortex in the different experimental groups. (A–H) Control groups showing normal cortical architecture: (A, B) Control water (CW); (C, D) Control solvent extract (CSE); (E, F) Control ethanolic extract (CEE); (G, H) Control betanin (CBT). (I, J) prenatally VPA-exposed and postnatally water-treated group (VPA/W) showing numerous dark neurons with neuronophagia (arrows). (K, L) Prenatally VPA-exposed and postnatally solvent extract-treated group (VPA/SE) also displays numerous dark neurons with neuronophagia (arrows). (M, N) Prenatally VPA-exposed and postnatally ethanolic extract-treated group (VPA/EE) showing few degenerating neurons (arrows). (O, P) Prenatally VPA-exposed and postnatally betanin-treated group (VPA/BT) showing few degenerating neurons (arrows)

Furthermore, in Fig. 13 (I and J), the cerebellum displayed an increased number of necrotic Purkinje cells. In the VPA/SE group, Fig. 10 (K and L) revealed numerous degenerating dark neurons in the cerebral cortex. Although the hippocampus appeared slightly affected in Fig. 12 (G-L), the cerebellum in Fig. 13 (K and L) continued to exhibit considerable Purkinje cell degeneration. Conversely, the VPA/EE group demonstrated marked histological improvement across all brain regions. Brain sections showed only a few dark neurons in the cerebral cortex (Fig. 10 M and N), while the hippocampus appeared histologically normal (Fig. 12 M-R). The cerebellum exhibited minimal degeneration, with only occasional dark Purkinje cells noted (Fig. 13 M and N). Similarly, the VPA/BT group also exhibited notable improvement. The cerebral cortex contained few degenerating neurons (Fig. 10 O and P), the hippocampus appeared histologically intact (Fig. 12 S-Y), and the cerebellum showed only some degenerating Purkinje cells (Fig. 13 O and P).

Degenerated neurons were quantified in the cerebral cortex, hippocampus, and cerebellum of male rat pups across experimental groups (Fig. 14). In all brain regions, the VPA/W group showed a significant increase in neuronal degeneration compared with all control groups (CW,

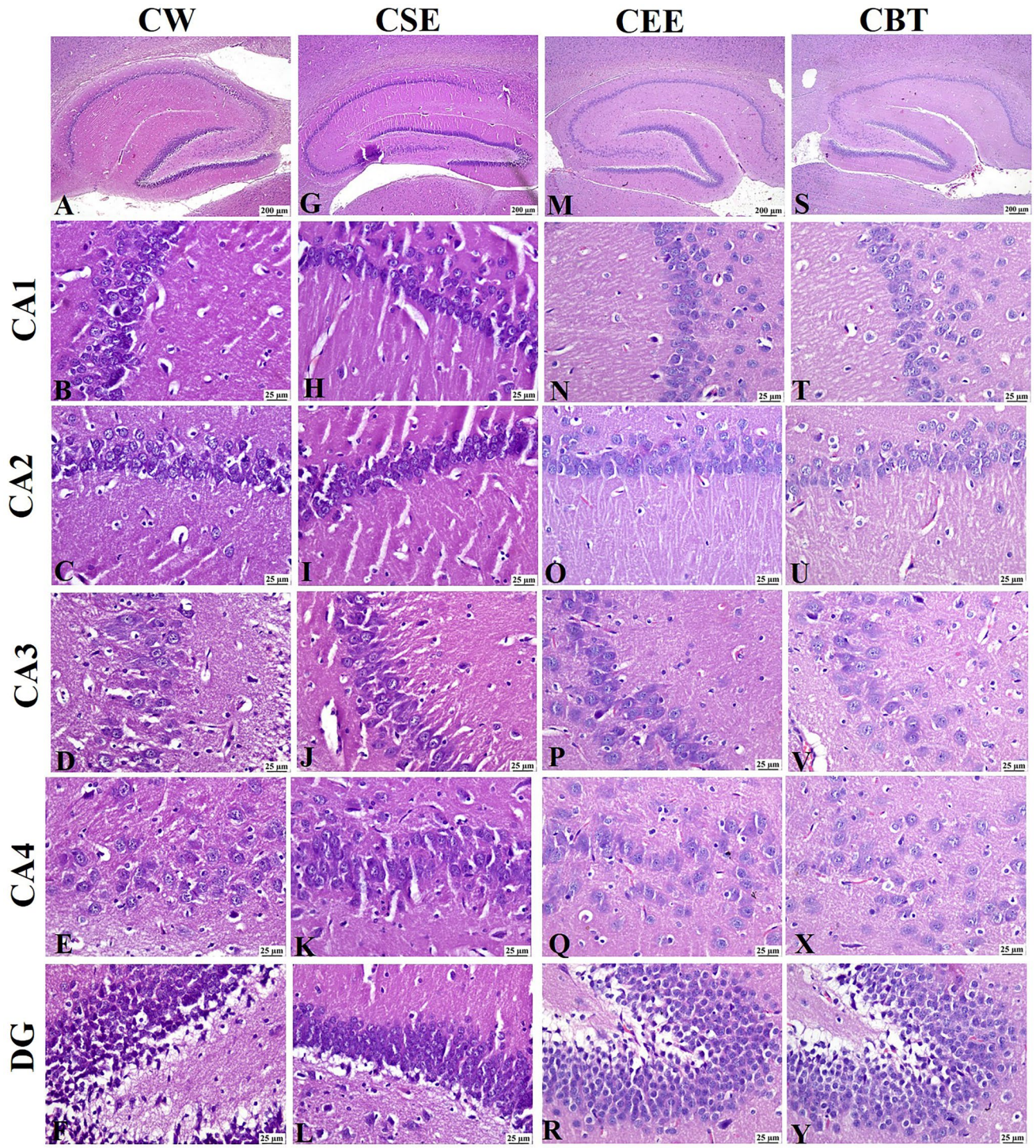


Fig. 11 Representative photomicrographs of hippocampal subregions (CA1, CA2, CA3, CA4, and dentate gyrus [DG]) with normal architecture and preserved neuronal layering and cell density in experimental control groups. (A-F) Control water (CW); (G-L) Control solvent extract (CSE); (M-R) Control ethanolic extract (CEE); and (S-Y) Control betanin (CBT)

CSE, CEE, and CBT; $p < 0.0001$). In the cerebral cortex (Fig. 14A), VPA/W exhibited the highest degeneration scores, whereas VPA/EE and VPA/BT showed significantly reduced degeneration (all $p < 0.01$ vs. VPA/W). A similar pattern was observed in the hippocampus (Fig. 14B), where VPA/W had significantly elevated degeneration ($p < 0.0001$), and VPA/EE and VPA/BT showed partial but significant protection ($p < 0.01$ and $p < 0.05$, respectively). In the

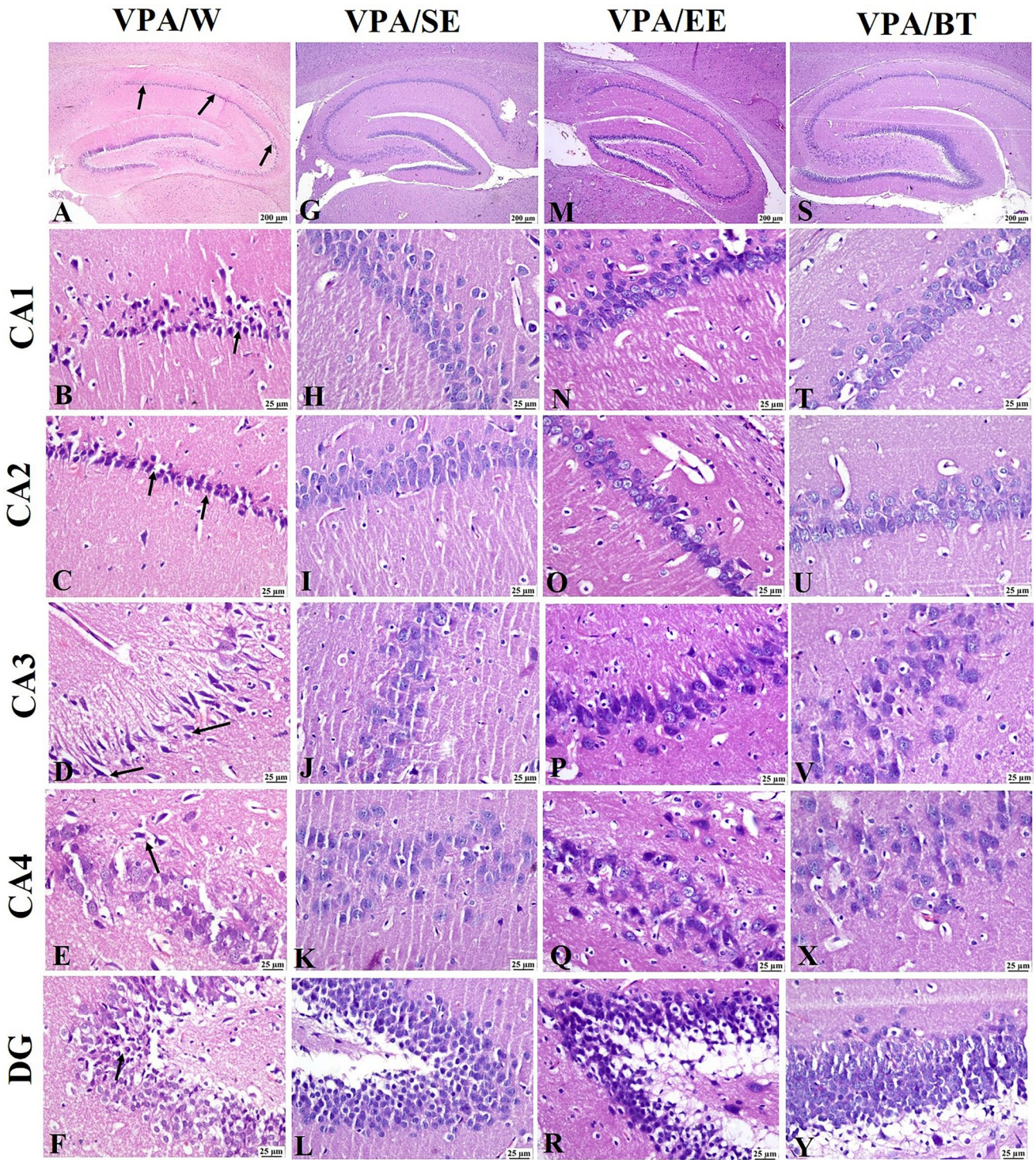


Fig. 12 Representative photomicrographs of hippocampal subregions (CA1, CA2, CA3, CA4, and dentate gyrus [DG]) in different experimental groups. (A–F) Prenatally VPA-exposed and postnatally water-treated group (VPA/W) showing severe neuronal loss, disrupted pyramidal layers, and diminished granule cells in DG (arrows). (G–L) Prenatally VPA-exposed and postnatally solvent extract-treated group (VPA/SE) showing partial preservation of hippocampal architecture with moderate neuronal damage. (M–R) Prenatally VPA-exposed and postnatally ethanolic extract-treated group (VPA/EE) showing normal architecture with preserved neuronal layering and cell density. (S–Y) Prenatally VPA-exposed and postnatally betanin-treated group (VPA/BT) showing marked improvement in histoarchitecture with nearly normal hippocampal layers and higher neuronal density

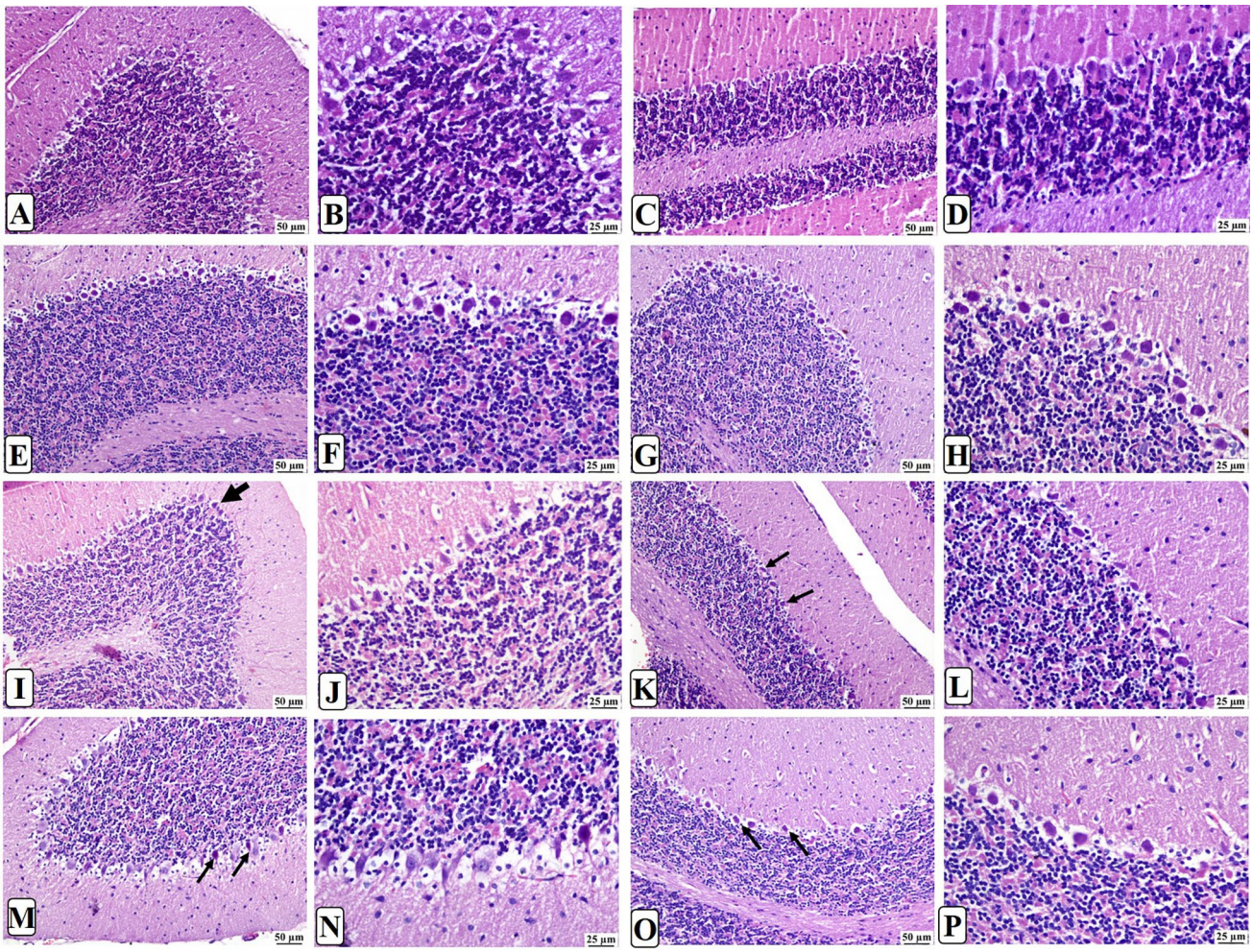


Fig. 13 Representative photomicrographs of the cerebellum in the different experimental groups. (A–H) Control groups showing normal cortical architecture: (A, B) Control water (CW); (C, D) Control solvent extract (CSE); (E, F) Control ethanolic extract (CEE); (G, H) Control betanin (CBT). (I, J) Prenatally VPA-exposed and postnatally water-treated group (VPA/W) showing numerous degenerating Purkinje cells (arrows). (K, L) Prenatally VPA-exposed and postnatally solvent extract-treated group (VPA/SE) also displays numerous degenerating Purkinje cells (arrows). (M, N) Prenatally VPA-exposed and postnatally ethanolic extract-treated group (VPA/EE) showing few degenerating Purkinje cells (arrows). (O, P) Prenatally VPA-exposed and postnatally betanin-treated group (VPA/BT) showing few degenerating Purkinje cells (arrows)

cerebellum (Fig. 14C), degeneration was again highest in VPA/W, with VPA/SE, VPA/EE, and VPA/BT producing significant reductions ($p < 0.001$). All control groups showed no neuronal degeneration, with no significant differences among them ($p > 0.05$).

3.9 Gene Expression Analysis of the Reelin Gene in the Rat Brain Cerebral Cortex

The expression profile of the Reelin gene across the experimental groups reveals critical insights into the effects of VPA and the potential therapeutic benefits of red beet treatments (Fig. 15). In the control groups, Reelin expression was relatively low in CW and CSE, whereas the CEE group exhibited a marked upregulation, followed by the CBT group. In contrast, the VPA/W and VPA/SE groups showed a significant downregulation of Reelin expression compared to all control groups ($p < 0.0001$). Meanwhile, the VPA/EE and VPA/BT groups exhibited partial recovery of Reelin expression, with the VPA/EE group showing the greatest improvement.

4 Discussion

The present study demonstrated that both the ethanolic extract of *B. vulgaris* leaves and its major pigment, betanin, exert multifaceted neuroprotective effects in a VPA–induced rat model of autism. By integrating phytochemical

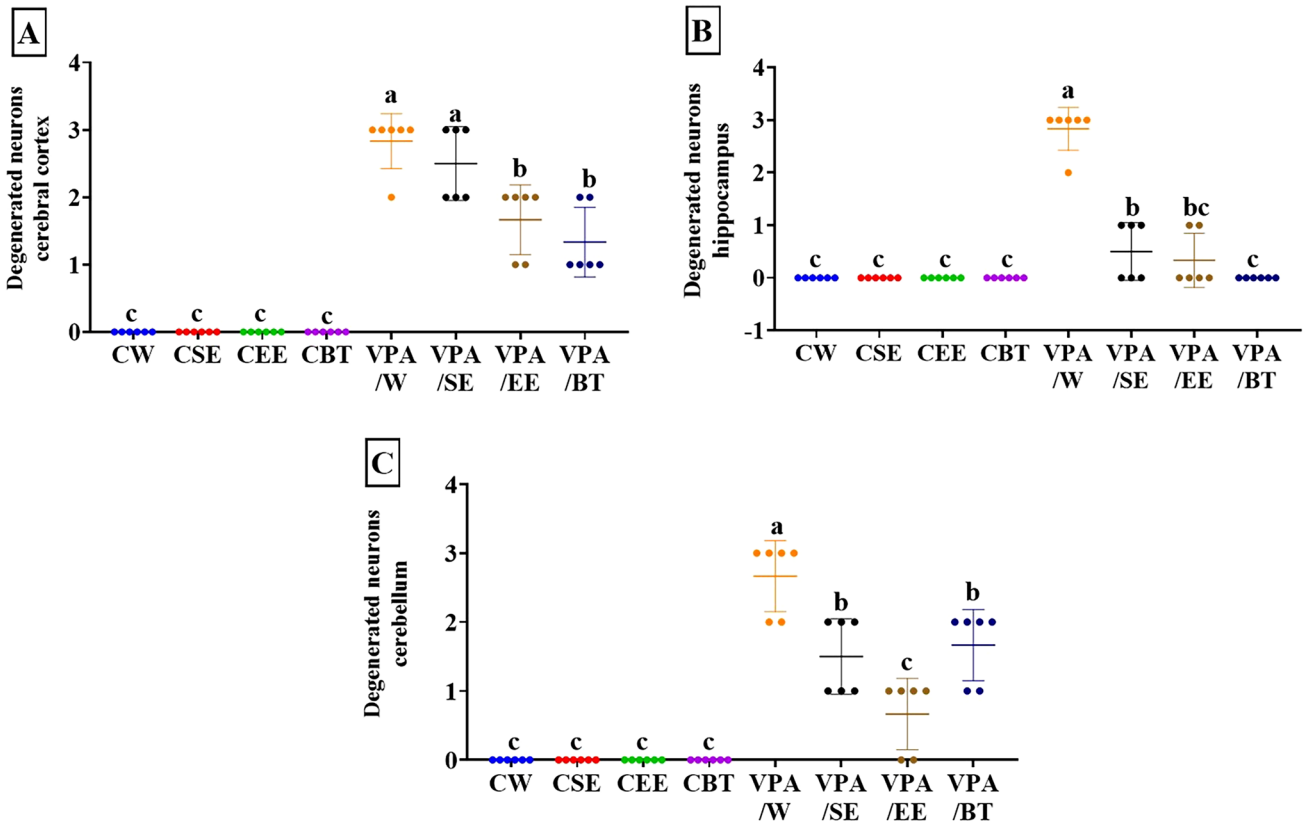


Fig. 14 Degenerated neurons lesion score in the (A) cerebral cortex, (B) hippocampus, and (C) cerebellum in different groups. Data are expressed as mean ± SE. $n = 6$. [a, b, and c] columns with different superscripts are statistically different at $P < 0.05$

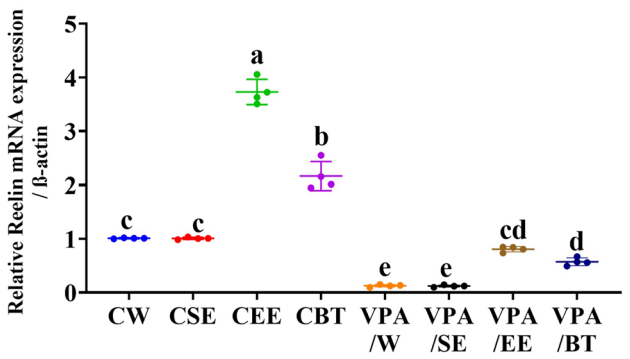


Fig. 15 Changes in mRNA expression of the Reelin gene in the cerebral cortex of valproic acid (VPA)-induced autistic rats and treatment groups. Control water (CW), control betanin (CBT), control solvent extract (CSE), control ethanolic extract (CEE), prenatally VPA-exposed and postnatally water-treated (VPA/W), prenatally VPA-exposed and postnatally solvent extract-treated (VPA/SE), prenatally VPA-exposed and postnatally ethanolic extract-treated (VPA/EE), and prenatally VPA-exposed and postnatally betanin-treated (VPA/BT). Data are expressed as mean ± SE. $n = 4$. [a, b, c, d, and e] columns with different superscripts are statistically different at $P < 0.05$

characterization, behavioral assays, neurochemical measurements, gene expression analysis, and histopathology, we identified several interrelated mechanisms through which these natural products can mitigate VPA's deleterious effects.

The rich antioxidant profile of the *B. vulgaris* extract, evidenced by moderate DPPH scavenging (IC_{50} ~ 125 µg/mL), high total phenolic (76 mg/g) and flavonoid (50 mg/g) contents, and the presence of potent polyphenols such as p-coumaric acid, gallic acid, cinnamic acid, and apigenin, likely underlies its capacity to restore redox homeostasis [19]. These compounds are known for their free radical scavenging, anti-apoptotic, and anti-inflammatory properties [56–60]. Betanin content (18.26 mg/g) was notably high, consistent with its known role as a potent antioxidant [61]. These findings provide a chemical basis for the neuroprotective effects observed in later experiments.

Prenatal exposure to VPA resulted in gross morphological deformities (e.g., tail kinking, spinal curvature), consistent with previous reports of developmental anomalies associated with ASD [62, 63]. These malformations are indicative of disrupted axial skeleton development, potentially due to interference with somitogenesis and neural tube closure during embryogenesis [63]. While some studies reported a

100% occurrence of tail kinks in VPA-exposed offspring [64, 65], others observed a markedly lower incidence [43, 66]. In our study, approximately 40% of the offspring exhibited tail kinks, further confirming the teratogenic impact of VPA. The gross morphological abnormalities observed here are consistent with previous reports of VPA-induced developmental defects in animal models [67, 68]. Moreover, VPA exposure in humans has been associated with neural tube defects such as spina bifida, underscoring the translational relevance of our findings and supporting the conserved teratogenic potential of VPA across species [7, 69, 70]. Hence, the observed defects support the validity of the VPA model in simulating developmental anomalies associated with ASD [71].

Behaviorally, VPA-exposed pups displayed significant impairments in SI and SNI in the three-chamber sociability test, core features of ASD [9]. These results are consistent with previous reports indicating social impairments and stereotypical behaviors in VPA-induced autism models [71, 72]. This could be highly related to the recorded decrease in cortical GABA levels in the AU group [73]. Autism is frequently associated with excitatory/inhibitory imbalance, particularly GABAergic dysfunction [74, 75]. GABA plays a significant role in enhancing social behavior through various neural mechanisms [76]. GABAergic neurons in the lateral septum enhance social preferences and novelty behaviors through projections to the ventral CA1 region. Activation of these neurons has been shown to enhance social interactions, while their inhibition can lead to social deficits [77]. The widespread presence of dark neurons across the CA1 region, along with pronounced neuronal loss in the hippocampus of the AU group, confirms this pathophysiology. On the contrary, the VPA/BT group showed fully restored and even enhanced SI and SNI scores beyond control levels, suggesting strong neuromodulatory potential. VPA/EE also improved behavior, although to a slightly lesser extent, indicating the therapeutic synergy of its constituents. In this respect, VPA/BT restored GABA concentrations to near-control levels, suggesting either upregulation of GABA synthesis (e.g., glutamate decarboxylase activity) or reduced degradation. EE also had a significant effect, although less pronounced, possibly due to a more complex interaction of phytochemicals. Restoration of GABAergic tone likely underlies the behavioral improvements and may also contribute to reduced seizure susceptibility. Similarly, in a study on rats exposed to GABA, a positive allosteric modulator of GABA A receptors improved sociability and cognitive function, suggesting therapeutic potential for GABAergic modulation in ASD [78]. Another important aspect is that Shi, Yan [79] reported the inhibitory inputs from the hippocampal CA1 to the retrosplenial cortex are essential for normal social behavior and can rescue social deficits in ASD models. Hence, the restoration of the normal architecture of the CA1 region, along with the increased GABA concentration observed in both the VPA/BT and VPA/EE groups, may underlie the enhancement of social behavior in these groups. Importantly, betanin and *B. vulgaris* extract exhibits significant antioxidant and anti-inflammatory properties, which may contribute to better emotional regulation, potentially fostering more positive social interactions [80, 81].

Oxidative stress is a key driver of neurodevelopmental damage in ASD [82]. VPA exposure significantly elevated MDA (a lipid peroxidation marker) and suppressed antioxidant defenses (GSH and CAT). These changes point to compromised antioxidant defenses and lipid peroxidation of neuronal membranes, reinforcing previous findings by Chaudhary and Parvez [83] and Aranarochana, Sirichoat [84]. Histological examination confirmed the biochemical and behavioral findings. VPA exposure caused extensive neurodegeneration across critical brain regions, including the cerebral cortex, cerebellum, and hippocampus, regions consistently implicated in ASD [85, 86]. The cerebral cortex showed signs of cytoarchitectural disruption, including shrunken, irregularly shaped neurons. In the cerebellum, Purkinje and granular cells, essential for motor and cognitive functions, were particularly vulnerable, corroborating earlier findings [87, 88]. The hippocampus, particularly the CA1-CA4 regions and dentate gyrus, displayed obvious neurodegeneration. On the contrary, both VPA/BT and VPA/EE reversed these alterations, restoring redox balance. Similarly, betanin diminished the oxidative burden of ischemia induced experimentally in animal brains and managed to support the hippocampus integrity by its strong antioxidant capacity and kept a high level of catalase activity [89]. The antioxidant efficacy of betanin is well documented and likely mediated through the enhancement of endogenous antioxidant enzymes and scavenging of free radicals [90]. The comparable efficacy of VPA/EE implies additional contributions from phenolics and flavonoids, including those that may act through Nrf2 activation or direct ROS quenching [91, 92]. By quelling oxidative damage, VPA/BT and VPA/EE treatments preserve neuronal viability, as reflected in preserved histoarchitecture, reducing neuronophagia, dark neuron formation, and Purkinje cell loss in the cortex, hippocampus, and cerebellum, corroborating their neuroprotective effects. Similarly, betanin has been reported to prevent neuronal death through counteraction of inflammatory cytokines, oxidative stress, and apoptosis [93]. These structural findings dovetail with the biochemical and molecular data, painting a coherent picture of how antioxidant, anti-inflammatory, anti-apoptotic, and gene-regulatory activities converge to prevent VPA-induced neuropathology.

Neuroinflammation, particularly TNF-α elevation, is a hallmark of autism [82] and was significantly increased in the VPA/W group. Treatment with VPA/BT and VPA/EE reduced TNF-α levels, indicating a strong anti-inflammatory

response. This is consistent with the known ability of betalains and flavonoids to suppress pro-inflammatory cytokines via inhibition of NF-κB and MAPK pathways [94, 95]. The reduction in TNF-α likely contributes to both improved neuronal survival and functional outcomes [96, 97]. Similarly, a study by Albasher, Alsaleh [98] highlighted that red beet extract significantly protected cortical neurons from chlorpyrifos-induced toxicity through its anti-inflammatory and anti-apoptotic activities.

Apoptotic dysregulation is implicated in the neuropathology of ASD [13]. The decrease in anti-apoptotic BCL2 and increase in pro-apoptotic caspase-3 in the VPA/W group reflect enhanced neuronal loss [99]. Both VPA/BT and VPA/EE reversed these changes, reinforcing anti-apoptotic signaling. Betanin has been shown to upregulate BCL2 and inhibit mitochondrial cytochrome c release, while polyphenols can directly interfere with caspase activation. Hence, by preserving mitochondrial integrity and inhibiting the intrinsic apoptotic pathway, these compounds enhance neuronal survival.

At the molecular level, our results highlight downregulation of the Reelin gene in VPA-exposed rats. Given Reelin's vital role in neuronal migration, cortical layering, and synaptic plasticity [15, 100], its suppression may contribute to the disorganized brain architecture observed in ASD. Reelin is released from a specific GABAergic interneuron and also released from a population of cells in the developing cerebral cortex marginal zone referred to as the Cajal-Retzius cells [101]. Beyond early development, Reelin remains active in adulthood, where it contributes to the strengthening of synaptic connections and the regulation of neuronal communication, processes essential for memory formation and learning [102]. Given its critical role in neurodevelopment, altered Reelin expression has been strongly associated with ASD and other neuropsychiatric conditions [15]. Both VPA/BT and VPA/EE significantly restored Reelin expression, with VPA/EE being more effective, suggesting a novel mechanism for its neurodevelopmental benefits. This observation aligns with previous reports linking natural bioactive agents, such as apitoxin, with upregulation of Reelin expression and neuroprotection [103]. The superiority of VPA/EE over VPA/BT on the modulation of Reelin gene expression may stem from the broader epigenetic and transcriptional regulatory potential of the synergistic actions of multiple phytochemicals in the full extract. Polyphenols are known to modulate DNA methylation and histone acetylation [104], which could alleviate VPA-induced epigenetic suppression of the Reelin gene. Restored Reelin expression would facilitate proper cortical layering and synaptic connectivity, aligning with the improved histology and behaviors observed.

5 Conclusion

Taken together, our results suggest that *B. vulgaris* leaf extract and its principal pigment, betanin, provide robust neuroprotection in a VPA-induced autism model. This protection appears to occur through complementary mechanisms, including restoration of antioxidant defenses, anti-inflammatory activity, normalization of GABAergic neurotransmission, inhibition of apoptosis, upregulation of neurodevelopmental genes, and preservation of histological architecture. Betanin's more pronounced effects on GABA and sociability hint at possible direct neuromodulatory actions, whereas the full extract's superiority in restoring Reelin implies epigenetic and multi-target phytochemical synergy. Future work should dissect these pathways in greater molecular detail, including epigenetic profiling, receptor binding studies, and metabolomic analyses, explore optimal dosing regimens, and validate these effects in clinical settings. Ultimately, these findings support further investigation of red beet-derived nutraceuticals as adjunctive therapies for neurodevelopmental disorders.

Author Contribution Nada S. Al-wakeel: conceptualization, methodology, formal analysis, investigation, resources, writing—original draft. Manar E. Selim: conceptualization, methodology, investigation, data curation, supervision, writing—review and editing. Yasmina M. Abd-Elhakim: conceptualization, formal analysis, data curation, visualization, supervision, writing—review and editing. Manal M. Hefny: conceptualization, investigation, supervision, writing—review and editing. All authors have read and agreed to the published version of the manuscript.

Funding Open access funding provided by The Science, Technology & Innovation Funding Authority (STDF) in cooperation with The Egyptian Knowledge Bank (EKB). The authors declare that no funds, grants, or other support were received during the preparation of this manuscript.

Data Availability Data will be made available on request.

Declarations

Conflict of interest The authors declare no competing interests.

Ethical Approval The experiment was conducted per the ethical recommendations for the Use and Care of Laboratory Animals in scientific investigations set by the National Institutes of Health (NIH), and it was supervised by the Animal Use in Research Committee of Ain Shams University (Approval number ASU-SCI/ZOOL/2025/6/4).

Clinical Trial Number Not applicable.

Consent to Participate All authors have participated in this work.

Consent for Publication All authors reviewed and approved the manuscript for publication.

Open Access This article is licensed under a Creative Commons Attribution 4.0 International License, which permits use, sharing, adaptation, distribution and reproduction in any medium or format, as long as you give appropriate credit to the original author(s) and the source, provide a link to the Creative Commons licence, and indicate if changes were made. The images or other third party material in this article are included in the article's Creative Commons licence, unless indicated otherwise in a credit line to the material. If material is not included in the article's Creative Commons licence and your intended use is not permitted by statutory regulation or exceeds the permitted use, you will need to obtain permission directly from the copyright holder. To view a copy of this licence, visit http://creativecommons.org/licenses/by/4.0/.

References

1. Anisman H, Hayley S, Kusnecov A. Chapter 13 - Autism. In: Anisman H, Hayley S, Kusnecov A, editors. The Immune System (Second Edition): Academic Press; 2025. p. 345–64.
2. Zeidan J, Fombonne E, Scorah J, Ibrahim A, Durkin MS, Saxena S, et al. Global prevalence of autism: a systematic review update. Autism Res. 2022;15(5):778–90. https://doi.org/10.1002/aur.2696.
3. Loomes R, Hull L, Mandy WPL. What is the male-to-female ratio in Autism Spectrum Disorder? A systematic review and meta-analysis. J Am Acad Child Adolesc Psychiatry. 2017;56(6):466–74. https://doi.org/10.1016/j.jaac.2017.03.013.
4. Shaw KA. Prevalence and early identification of autism spectrum disorder among children aged 4 and 8 years-Autism and Developmental Disabilities Monitoring Network, 16 sites, United States, 2022. MMWR Surveill Summ. 2025. https://doi.org/10.15585/mmwr.ss7402a1.
5. Lazar SM, Challman TD, Myers SM. Etiologic evaluation of children with Autism Spectrum Disorder. Pediatr Clin North Am. 2024;71(2):179–97. https://doi.org/10.1016/j.pcl.2023.12.002.
6. Wiggs KK, Rickert ME, Sujan AC, Quinn PD, Larsson H, Lichtenstein P, et al. Antiseizure medication use during pregnancy and risk of ASD and ADHD in children. Neurology. 2020;95(24):e3232–40. https://doi.org/10.1212/WNL.0000000000001099.
7. Jentink J, Loane MA, Dolk H, Barisic I, Garne E, Morris JK, et al. Valproic acid monotherapy in pregnancy and major congenital malformations. N Engl J Med. 2010;362(23):2185–93. https://doi.org/10.1056/NEJMoa0907328.
8. Nicolini C, Fahnestock M. The valproic acid-induced rodent model of autism. Exp Neurol. 2018;299:217–27. https://doi.org/10.1016/j.expneurol.2017.04.017.
9. Szabó J, Renczés E, Borbélyová V, Ostatníková D, Celec P. Assessing sociability using the Three-Chamber Social Interaction Test and the Reciprocal Interaction Test in a genetic mouse model of ASD. Behav Brain Funct. 2024;20(1):24. https://doi.org/10.1186/s12993-024-00251-0.
10. Chaliha D, Albrecht M, Vaccarezza M, Takechi R, Lam V, Al-Salami H, et al. A systematic review of the valproic-acid-induced rodent model of autism. Dev Neurosci. 2020;42(1):12–48. https://doi.org/10.1159/000509109.
11. Luhach K, Kulkarni GT, Singh VP, Sharma B. Vinpocetine amended prenatal valproic acid induced features of ASD possibly by altering markers of neuronal function, inflammation, and oxidative stress. Autism Res. 2021;14(11):2270–86. https://doi.org/10.1002/aur.2597.
12. Liu X, Lin J, Zhang H, Khan NU, Zhang J, Tang X, et al. Oxidative stress in Autism Spectrum Disorder-current progress of mechanisms and biomarkers. Front Psychiatry. 2022;13:813304. https://doi.org/10.3389/fpsyt.2022.813304.
13. Jian J, Li L-G, Zhao P-J, Zheng R-J, Dong X-W, Zhao Y-H, et al. Mouse nerve growth factor suppresses neuronal apoptosis in valproic acid-induced Autism Spectrum Disorder rats by regulating the phosphoinositide-3-kinase/serine/threonine kinase signaling pathway. Pharmacogenet Genomics. 2023;33(5):101–10. https://doi.org/10.1097/FPC.0000000000000498.
14. Hooshmandi M, Wong C, Khoutorsky A. Dysregulation of translational control signaling in Autism Spectrum Disorders. Cell Signal. 2020;75:109746. https://doi.org/10.1016/j.cellsig.2020.109746.
15. Scala M, Grasso EA, Di Cara G, Riva A, Striano P, Verrotti A. The pathophysiological link between Reelin and Autism: overview and new insights. Front Genet. 2022;13:869002. https://doi.org/10.3389/fgene.2022.869002.
16. Sivasangari K, Rajan KE. Prenatal exposure to valproic acid alters Reelin, NGF expressing neuron architecture and impairs social interaction in their autistic-like phenotype male offspring. Exp Brain Res. 2022;240(7):2005–16. https://doi.org/10.1007/s00221-022-06386-8.
17. Doherty M, Foley K-R, Schloss J. Complementary and alternative medicine for Autism – a systematic review. J Autism Dev Disord. 2024. https://doi.org/10.1007/s10803-024-06449-5.
18. Thiruvengadam M, Chung I-M, Samynathan R, Chandar SH, Venkidasamy B, Sarkar T, et al. A comprehensive review of beetroot (**Beta vulgaris** L.) bioactive components in the food and pharmaceutical industries. Crit Rev Food Sci Nutr. 2024;64(3):708–39. https://doi.org/10.1080/10408398.2022.2108367.
19. Almeida D, Petropoulos SA, da Silveira TFF, Pires T, Ferreira I, Fernandes Â, et al. Exploring the biochemical profile of **Beta vulgaris** L.: A comparative study of beetroots and Swiss chard. Plants. 2025. https://doi.org/10.3390/plants14040591.
20. Spórna-Kucab A, Tekieli A, Grzegorczyk A, Świątek Ł, Boguszewska A, Skalicka-Woźniak K. Betaxanthin profiling in relation to the biological activities of red and yellow *Beta vulgaris* L. extracts. Metabolites. 2023;13(3):408. https://doi.org/10.3390/metabo13030408.
21. Ravichandran K, Smetanska I, Antony U. Chapter 19 - Red beet. In: Jaiswal AK, editor. Nutritional Composition and Antioxidant Properties of Fruits and Vegetables: Academic Press; 2020. p. 315–21.
22. Szymański J, Szwajgier D, Baranowska-Wójcik E. The role of beetroot ingredients in the prevention of Alzheimer's Disease. Appl Sci Basel. 2023;13(2):1044. https://doi.org/10.3390/app13021044.
23. Esquivel P. Chapter 6 - Betalains. In: Schweiggert R, editor. Handbook on Natural Pigments in Food and Beverages (Second Edition): Woodhead Publishing; 2024. p. 147–67.
24. Spiegel M, Gamian A, Sroka Z. Antiradical activity of beetroot (**Beta vulgaris** L.) betalains. Molecules. 2021;26(9):2439. https://doi.org/10.3390/molecules26092439.
25. Ştefănescu C, Voştinaru O, Mogoşan C, Crişan G, Balica G. The neuroprotective potential of betalains: a focused review. Plants Basel. 2025;14(7):994. https://doi.org/10.3390/plants14070994.
26. Thong-Asa W, Puenpha K, Lairaksa T, Saengjinda S. Neuroprotective effects of betanin in mice with cerebral ischemia-reperfusion injury. Exp Anim. 2023;72(3):336–45. https://doi.org/10.1538/expanim.22-0176.
27. Rahimi P, Abedimanesh S, Mesbah-Namin SA, Ostadrahimi A. Betalains, the nature-inspired pigments, in health and diseases. Crit Rev Food Sci Nutr. 2019;59(18):2949–78. https://doi.org/10.1080/10408398.2018.1479830.
28. Pinheiro VdS, Junior OJFR, Ortmann CF, Pande A, Conte-Junior CA, Alvares TS. Evaluation of 12-week standardized beetroot extract supplementation in older participants: a preliminary study

of human health safety. Nutrients. 2024;16(12):1942. https://doi.org/10.3390/nu16121942.
29. Khan MI, Joseph KD, Ramesh HP, Giridhar P, Ravishankar GA. Acute, subacute and subchronic safety assessment of betalains rich *Rivina humilis* L. berry juice in rats. Food Chem Toxicol. 2011;49(12):3154–7. https://doi.org/10.1016/j.fct.2011.08.022.
30. Martinez RM, Melo CPB, Pinto IC, Mendes-Pierotti S, Vignoli JA, Verri WA, et al. Betalains: a narrative review on pharmacological mechanisms supporting the nutraceutical potential towards health benefits. Foods. 2024;13(23):3909. https://doi.org/10.3390/foods13233909.
31. Khan MI. Plant Betalains: safety, antioxidant activity, clinical efficacy, and bioavailability. Compr Rev Food Sci Food Saf. 2016;15(2):316–30. https://doi.org/10.1111/1541-4337.12185.
32. Ebrahimi P, Mihaylova D, Marangon CM, Grigoletto L, Lante A. Impact of sample pretreatment and extraction methods on the bioactive compounds of sugar beet (**Beta vulgaris** L.) leaves. Molecules. 2022;27(22):8110. https://doi.org/10.3390/molecules27228110.
33. Yen GC, Duh PD. Scavenging effect of methanolic extracts of peanut hulls on free-radical and active-oxygen species. J Agric Food Chem. 1994;42(3):629–32.
34. Al Zahrani NA, El-Shishtawy RM, Elaasser MM, Asiri AM. Synthesis of novel chalcone-based phenothiazine derivatives as antioxidant and anticancer agents. Molecules. 2020;25(19):4566. https://doi.org/10.3390/molecules25194566.
35. Singleton VL, Orthofer R, Lamuela-Raventós RM. [14] Analysis of total phenols and other oxidation substrates and antioxidants by means of folin-ciocalteu reagent. Methods in enzymology. 299: Elsevier; 1999. p. 152–78.
36. Chang C-C, Yang M-H, Wen H-M, Chern J-C. Estimation of total flavonoid content in propolis by two complementary colorimetric methods. J Food Drug Anal. 2002. https://doi.org/10.38212/2224-6614.2748.
37. Lin Y-L, Juan I-M, Chen Y-L, Liang Y-C, Lin J-K. Composition of polyphenols in fresh tea leaves and associations of their oxygen-radical-absorbing capacity with antiproliferative actions in fibroblast cells. J Agric Food Chem. 1996;44(6):1387–94. https://doi.org/10.1021/jf950652k.
38. Kuntić V, Pejić N, Ivković B, Vujić Z, Ilić K, Mićić S, et al. Isocratic RP-HPLC method for rutin determination in solid oral dosage forms. J Pharm Biomed Anal. 2007;43(2):718–21. https://doi.org/10.1016/j.jpba.2006.07.019.
39. Cezar LC, Kirsten TB, da Fonseca CCN, de Lima APN, Bernardi MM, Felicio LF. Zinc as a therapy in a rat model of autism prenatally induced by valproic acid. Prog Neuro-Psychopharmacol Biol Psychiatry. 2018;84:173–80. https://doi.org/10.1016/j.pnpbp.2018.02.008.
40. Cusmano DM, Mong JA. In utero exposure to valproic acid changes sleep in juvenile rats: a model for sleep disturbances in autism. Sleep. 2014;37(9):1489–99. https://doi.org/10.5665/sleep.3998.
41. Cohen OS, Varlinskaya EI, Wilson CA, Glatt SJ, Mooney SM. Acute prenatal exposure to a moderate dose of valproic acid increases social behavior and alters gene expression in rats. Int J Dev Neurosci. 2013;31(8):740–50. https://doi.org/10.1016/j.ijdevneu.2013.09.002.
42. Wellmann KA, Varlinskaya EI, Mooney SM. D-Cycloserine ameliorates social alterations that result from prenatal exposure to valproic acid. Brain Res Bull. 2014;108:1–9. https://doi.org/10.1016/j.brainresbull.2014.08.001.
43. Favre MR, Barkat TR, Mendola DL, Khazen G, Markram H, Markram K. General developmental health in the VPA-rat model of autism. Front Behav Neurosci. 2013. https://doi.org/10.3389/fnbeh.2013.00088.
44. Tunçak S, Gören B, Uzbay T, Öz P. Assessment of empathy-like behaviour in Valproic Acid–induced rat model of autism. Int J Dev Neurosci. 2025;85(2):e70008. https://doi.org/10.1002/jdn.70008.
45. Abd El-Ghffar EA, Hegazi NM, Saad HH, Soliman MM, El-Raey MA, Shehata SM, et al. HPLC-ESI-MS/MS analysis of beet (*Beta vulgaris*) leaves and its beneficial properties in type 1 diabetic rats. Biomed Pharmacother. 2019;120:109541. https://doi.org/10.1016/j.biopha.2019.109541.
46. Tan D, Wang Y, Bai B, Yang X, Han J. Betanin attenuates oxidative stress and inflammatory reaction in kidney of paraquat-treated rat. Food Chem Toxicol. 2015;78:141–6. https://doi.org/10.1016/j.fct.2015.01.018.
47. Kim KC, Kim P, Go HS, Choi CS, Yang S-I, Cheong JH, et al. The critical period of valproate exposure to induce autistic symptoms in Sprague–Dawley rats. Toxicol Lett. 2011;201(2):137–42. https://doi.org/10.1016/j.toxlet.2010.12.018.
48. Bambini-Junior V, Zanatta G, Nunes GDF, de Melo GM, Michels M, Fontes-Dutra M, et al. Resveratrol prevents social deficits in animal model of autism induced by valproic acid. Neurosci lett. 2014;583:176–81. https://doi.org/10.1016/j.ibneur.2023.09.008.
49. Beutler E, Mary KY. Erythrocyte glutathione reductase. Blood. 1963;21(5):573–85.
50. Aebi H. [13] Catalase in vitro. Methods in enzymology. 105: Elsevier; 1984. p. 121–6.
51. Ohkawa H, Ohishi N, Yagi K. Assay for lipid peroxides in animal tissues by thiobarbituric acid reaction. Anal Biochem. 1979;95(2):351–8.
52. Banni M, Messaoudi I, Said L, El Heni J, Kerkeni A, Said K. Metallothionein gene expression in liver of rats exposed to cadmium and supplemented with zinc and selenium. Arch Environ Contam Toxicol. 2010;59(3):513–9. https://doi.org/10.1007/s00244-010-9494-5.
53. Sui L, Ren W-W, Li B-M. Administration of thyroid hormone increases reelin and brain-derived neurotrophic factor expression in rat hippocampus in vivo. Brain Res. 2010;1313:9–24. https://doi.org/10.1016/j.brainres.2009.12.010.
54. Livak KJ, Schmittgen TD. Analysis of relative gene expression data using real-time quantitative PCR and the 2(-Delta Delta C(T)) method. Methods (San Diego, Calif). 2001;25(4):402–8.
55. Suvarna KS, Layton C, Bancroft JD. Bancroft's theory and practice of histological techniques: Elsevier health sciences; 2018.
56. Abo-El-Sooud K, Abd-El Hakim YM, Hashem MMM, El-Metwally AE, Hassan BA, El-Nour HHM. Restorative effects of gallic acid against sub-chronic hepatic toxicity of co-exposure to zinc oxide nanoparticles and arsenic trioxide in male rats. Heliyon. 2023. https://doi.org/10.1016/j.heliyon.2023.e17326.
57. Pontiki E, Hadjipavlou-Litina D. Multi-target cinnamic acids for oxidative stress and inflammation: Design, synthesis, biological evaluation and modeling studies. Molecules. 2019;24(1):12. https://doi.org/10.3390/molecules24010012.
58. Chen F, Zhang X, Wang J, Wang F, Mao J. P-coumaric acid: advances in pharmacological research based on oxidative stress. Curr Top Med Chem. 2024;24(5):416–36. https://doi.org/10.2174/0115680266276823231230183519.
59. Rahimi A, Alimohammadi M, Faramarzi F, Alizadeh-Navaei R, Rafiei A. The effects of apigenin administration on the inhibition of inflammatory responses and oxidative stress in the lung injury models: a systematic review and meta-analysis of preclinical evidence. Inflammopharmacology. 2022;30(4):1259–76. https://doi.org/10.1007/s10787-022-00994-0.
60. Zare MFR, Rakhshan K, Aboutaleb N, Nikbakht F, Naderi N, Bakhshesh M, et al. Apigenin attenuates doxorubicin induced cardiotoxicity via reducing oxidative stress and apoptosis in male rats. Life Sci. 2019;232:116623. https://doi.org/10.1016/j.lfs.2019.116623.

61. Silva DVTd, Baiao DdS, Ferreira VF, Paschoalin VMF. Betanin as a multipath oxidative stress and inflammation modulator: a beetroot pigment with protective effects on cardiovascular disease pathogenesis. Crit Rev Food Sci Nutr. 2021;62(2):539–54. https://doi.org/10.1080/10408398.2020.1822277.
62. Gao J, Wang X, Sun H, Cao Y, Liang S, Wang H, et al. Neuroprotective effects of docosahexaenoic acid on hippocampal cell death and learning and memory impairments in a valproic acid-induced rat autism model. Int J Dev Neurosci. 2016;49:67–78. https://doi.org/10.1016/j.ijdevneu.2015.11.006.
63. Saft P, Toledo-Cardenas R, Coria-Avila G, Perez-Pouchoulen M, Brug B, Hernandez M, et al. Characterization of four types of tail abnormalities in rats treated prenatally with valproic acid. Rev Eneurobiología. 2014;5(9).
64. Foley AG, Gannon S, Rombach-Mullan N, Prendergast A, Barry C, Cassidy AW, et al. Class I histone deacetylase inhibition ameliorates social cognition and cell adhesion molecule plasticity deficits in a rodent model of autism spectrum disorder. Neuropharmacology. 2012;63(4):750–60. https://doi.org/10.1016/j.neuropharm.2012.05.042.
65. Hou Q, Wang Y, Li Y, Chen D, Yang F, Wang S. A developmental study of abnormal behaviors and altered gabaergic signaling in the VPA-treated rat model of autism. Front Behav Neurosci. 2018;12:182. https://doi.org/10.3389/fnbeh.2018.00182.
66. Servadio M, Manduca A, Melancia F, Leboffe L, Schiavi S, Campolongo P, et al. Impaired repair of DNA damage is associated with autistic-like traits in rats prenatally exposed to valproic acid. Eur Neuropsychopharmacol. 2018;28(1):85–96. https://doi.org/10.1016/j.euroneuro.2017.11.014.
67. Alsdorf R, Wyszynski DF. Teratogenicity of sodium valproate. Expert Opin Drug Saf. 2005;4(2):345–53. https://doi.org/10.1517/14740338.4.2.345.
68. Schneider T, Przewłocki R. Behavioral alterations in rats prenatally exposed to valproic acid: animal model of autism. Neuropsychopharmacology. 2005;30(1):80–9. https://doi.org/10.1038/sj.npp.1300518.
69. Ornoy A. Valproic acid in pregnancy: How much are we endangering the embryo and fetus? Reprod Toxicol (Elmsford, NY). 2009;28(1):1–10. https://doi.org/10.1016/j.reprotox.2009.02.014.
70. Jentink J, Bakker MK, Nijenhuis CM, Wilffert B, de Jong- Berg LT. Does folic acid use decrease the risk for spina bifida after in utero exposure to valproic acid? Pharmacoepidemiol Drug Saf. 2010;19(8):803–7. https://doi.org/10.1002/pds.1975.
71. Elnahas EM, Abuelezz SA, Mohamad MI, Nabil MM, Abdelraouf SM, Bahaa N, et al. Validation of prenatal versus postnatal valproic acid rat models of autism: a behavioral and neurobiological study. Prog Neuro-Psychopharmacol Biol Psychiatry. 2021;108:110185. https://doi.org/10.1016/j.pnpbp.2020.110185.
72. Ferguson SA, Law CD, Abshire JS. Developmental treatment with bisphenol A causes few alterations on measures of postweaning activity and learning. Neurotoxicol Teratol. 2012;34(6):598–606. https://doi.org/10.1016/j.ntt.2012.09.006.
73. Lauber E, Filice F, Schwaller B. Prenatal valproate exposure differentially affects parvalbumin-expressing neurons and related circuits in the cortex and striatum of mice. Front Mol Neurosci. 2016;9:150. https://doi.org/10.3389/fnmol.2016.00150.
74. Sideraki A, Drigas A. GABA and executive functions in ASD. Sci Electron Arch. 2024. https://doi.org/10.36560/17320241940.
75. Park G, Jeon SJ, Ko IO, Park JH, Lee KC, Kim M-S, et al. Decreased in vivo glutamate/GABA ratio correlates with the social behavior deficit in a mouse model of autism spectrum disorder. Mol Brain. 2022;15(1):19. https://doi.org/10.1186/s13041-022-00904-z.
76. Paine TA, Swedlow N, Swetschinski L. Decreasing GABA function within the medial prefrontal cortex or basolateral amygdala decreases sociability. Behav Brain Res. 2017;317:542–52. https://doi.org/10.1016/j.bbr.2016.10.012.
77. Wang D, Zhao D, Wang W, Hu F, Cui M, Liu J, et al. How do lateral septum projections to the ventral CA1 influence sociability? Neural Regen Res. 2024;19(8):1789–801. https://doi.org/10.4103/1673-5374.389304.
78. Souza AJ, Freitas ÍS, Sharmin D, Cook JM, Guimarães FS, Gomes FV. An alpha 5-GABA(A) receptor positive allosteric modulator attenuates social and cognitive deficits without changing dopamine system hyperactivity in rats exposed to valproic acid in utero. Autism Res. 2024;17(8):1534–44. https://doi.org/10.1002/aur.3178.
79. Shi Y, Yan J, Xu X, Qiu Z. Gating of social behavior by inhibitory inputs from hippocampal CA1 to retrosplenial agranular cortex. Neurosci Bull. 2024;40(11):1635–48. https://doi.org/10.1007/s12264-023-01172-0.
80. Chen L, Zhu Y, Hu Z, Wu S, Jin C. Beetroot as a functional food with huge health benefits: antioxidant, antitumor, physical function, and chronic metabolomics activity. Food Sci Nutr. 2021;9(11):6406–20. https://doi.org/10.1002/fsn3.2577.
81. Salahinejad A, Attaran A, Meuthen D, Rachamalla M, Chivers DP, Niyogi S. Maternal exposure to bisphenol S induces neuropeptide signaling dysfunction and oxidative stress in the brain, and abnormal social behaviors in zebrafish (*Danio rerio*) offspring. Sci Total Environ. 2022;830:154794. https://doi.org/10.1016/j.scitotenv.2022.154794.
82. Usui N, Kobayashi H, Shimada S. Neuroinflammation and oxidative stress in the pathogenesis of autism spectrum disorder. Int J Mol Sci. 2023;24(6):5487. https://doi.org/10.3390/ijms24065487.
83. Chaudhary S, Parvez S. An in vitro approach to assess the neurotoxicity of valproic acid-induced oxidative stress in cerebellum and cerebral cortex of young rats. Neuroscience. 2012;225:258–68. https://doi.org/10.1016/j.neuroscience.2012.08.060.
84. Aranarochana A, Sirichoat A, Pannangrong W, Wigmore P, Welbat JU. Melatonin ameliorates valproic acid-induced neurogenesis impairment: the role of oxidative stress in adult rats. Oxid Med Cell Longev. 2021;2021(1):9997582. https://doi.org/10.1155/2021/9997582.
85. Varghese M, Keshav N, Jacot-Descombes S, Warda T, Wicinski B, Dickstein DL, et al. Autism spectrum disorder: neuropathology and animal models. Acta Neuropathol. 2017;134:537–66. https://doi.org/10.1007/s00401-017-1736-4.
86. Ornoy A, Weinstein-Fudim L, Tfilin M, Ergaz Z, Yanai J, Szyf M, et al. S-adenosyl methionine prevents ASD like behaviors triggered by early postnatal valproic acid exposure in very young mice. Neurotoxicol Teratol. 2019;71:64–74. https://doi.org/10.1016/j.ntt.2018.01.005.
87. Elgamal MA, Khodeer DM, Abdel-Wahab BA, Ibrahim IAA, Alzahrani AR, Moustafa YM, et al. Canagliflozin alleviates valproic acid-induced autism in rat pups: role of PTEN/PDK/PPAR-γ signaling pathways. Front Pharmacol. 2023;14:1113966. https://doi.org/10.3389/fphar.2023.1113966.
88. El-Baldem HT, Okasha EF, Elwan WM, Badr SM. Histological and immunohistochemical study of the possible protective effect of bee pollen extract on the cerebellar cortex of valproic acid-induced experimental model of autism in albino rat pups. Egypt J Cell Tissue Res. 2024;2(2):116–56. https://doi.org/10.21608/ejctr.2024.287099.1017.
89. Sakamula R, Thong-Asa W. Neuroprotective effect of p-coumaric acid in mice with cerebral ischemia reperfusion injuries. Metab Brain Dis. 2018;33:765–73. https://doi.org/10.1007/s11011-018-0185-7.

90. Thong-Asa W, Jedsadavitayakol S, Jutarattananon S. Benefits of betanin in rotenone-induced Parkinson mice. Metab Brain Dis. 2021;36(8):2567–77. https://doi.org/10.1007/s11011-021-00826-0.
91. Mittal A, Vashistha VK, Das DK. Free radical scavenging activity of gallic acid toward various reactive oxygen, nitrogen, and sulfur species: a DFT approach. Free Radic Res. 2023;57(2):81–90. https://doi.org/10.1080/10715762.2023.2197556.
92. Zheng Y-Z, Deng G, Zhang Y-C. Multiple free radical scavenging reactions of flavonoids. Dyes Pigments. 2022;198:109877. https://doi.org/10.1016/j.dyepig.2021.109877.
93. Thong-Asa W, Prasartsri S, Klomkleaw N, Thongwan N. The neuroprotective effect of betanin in trimethyltin-induced neurodegeneration in mice. Metab Brain Dis. 2020;35:1395–405. https://doi.org/10.1007/s11011-020-00615-1.
94. Moreno-Ley CM, Osorio-Revilla G, Hernández-Martínez DM, Ramos-Monroy OA, Gallardo-Velázquez T. Anti-inflammatory activity of betalains: a comprehensive review. Hum Nutr Metab. 2021;25:200126. https://doi.org/10.1016/j.hnm.2021.200126.
95. Tunon M, Garcia-Mediavilla M, Sanchez-Campos S, González-Gallego J. Potential of flavonoids as anti-inflammatory agents: modulation of pro-inflammatory gene expression and signal transduction pathways. Curr Drug Metab. 2009;10(3):256–71. https://doi.org/10.2174/138920009787846369.
96. Kim M, Jung K, Kim I-S, Lee I-S, Ko Y, Shin JE, et al. TNF-α induces human neural progenitor cell survival after oxygen–glucose deprivation by activating the NF-κB pathway. Exp Mol Med. 2018;50(4):1–14. https://doi.org/10.1038/s12276-018-0033-1.
97. Figiel I. Pro-inflammatory cytokine TNF-alpha as a neuroprotective agent in the brain. Acta Neurobiol Exp. 2008;68(4):526–34. https://doi.org/10.55782/ane-2008-1720.
98. Albasher G, Alsaleh AS, Alkubaisi N, Alfarraj S, Alkahtani S, Farhood M, et al. Red beetroot extract abrogates Chlorpyrifos-induced cortical damage in rats. Oxid Med Cell Longev. 2020;2020:2963020. https://doi.org/10.1155/2020/2963020.
99. Okouchi M, Ekshyyan O, Maracine M, Aw TY. Neuronal apoptosis in neurodegeneration. Antioxid Redox Signal. 2007;9(8):1059–96. https://doi.org/10.1089/ars.2007.1511.
100. Faini G, Del Bene F, Albadri S. Reelin functions beyond neuronal migration: from synaptogenesis to network activity modulation. Curr Opin Neurobiol. 2021;66:135–43. https://doi.org/10.1016/j.conb.2020.10.009.
101. Vílchez-Acosta A, Manso Y, Cárdenas A, Elias-Tersa A, Martínez-Losa M, Pascual M, et al. Specific contribution of Reelin expressed by Cajal–Retzius cells or GABAergic interneurons to cortical lamination. Proc Natl Acad Sci U S A. 2022;119(37):e2120079119. https://doi.org/10.1073/pnas.2120079119.
102. Levenson JM, Qiu S, Weeber EJ. The role of Reelin in adult synaptic function and the genetic and epigenetic regulation of the Reelin gene. Biochim et Biophy Acta (BBA) - Gene Regulatory Mech. 2008;1779(8):422–31. https://doi.org/10.1016/j.bbagrm.2008.01.001.
103. Daghestani MH, Selim ME, Abd-Elhakim YM, Said EN, El-Hameed NEA, Khalil SR, et al. The role of apitoxin in alleviating propionic acid-induced neurobehavioral impairments in rat pups: the expression pattern of Reelin gene. Biomed Pharmacother. 2017;93:48–56. https://doi.org/10.1016/j.biopha.2017.06.034.
104. Číž M, Dvořáková A, Skočková V, Kubala L. The role of dietary phenolic compounds in epigenetic modulation involved in inflammatory processes. Antioxidants Basel. 2020;9(8):691. https://doi.org/10.3390/antiox9080691.

Publisher's Note Springer Nature remains neutral with regard to jurisdictional claims in published maps and institutional affiliations.